Structural gonadal lesions observed in Japanese quail (*Coturnix coturnix japonica*) following exposure during puberty to the neonicotinoid pesticide, imidacloprid

Mohammed I.A. Ibrahim [a,*], Antoinette V. Lensink [b], Rephima M. Phaswane [a], Christo J. Botha [a]

[a] *Department of Paraclinical Sciences, Faculty of Veterinary Science, University of Pretoria, Onderstepoort 0110, South Africa*
[b] *Electron Microscope Unit, Department of Anatomy and Physiology, Faculty of Veterinary Sciences, University of Pretoria, Onderstepoort 0110, South Africa*

ABSTRACT

Exposure to the neonicotinoid insecticide, imidacloprid (IMI), causes reproductive toxicity in mammals and reptiles. However, reports on the effects of IMI on the gonads in birds are grossly lacking. Therefore, this study investigated the effects of pubertal exposure to IMI on the histology, ultrastructure, as well as the cytoskeletal proteins, desmin, smooth muscle actin and vimentin, of the gonads of Japanese quail (*Coturnix coturnix japonica*). Quails were randomly divided into four groups at 5 weeks of age. The control group was given only distilled water, whereas, the other three experimental groups, IMI was administered by oral gavage at 1.55, 3.1, and 6.2 mg/kg, twice per week for 4 weeks. Exposure to IMI doses of 3.1 and 6.2 mg/kg caused dose-dependent histopathological changes in the ovary and testis. In the ovary, accumulation of lymphocytes, degenerative changes, and necrosis with granulocyte infiltrations were observed, while in the testis, distorted seminiferous tubules, germ cell sloughing, vacuolisations, apoptotic bodies, autophagosomes, and mitochondrial damage were detected. These changes were accompanied by a decreased number of primary follicles ($P \leq 0.05$) in the ovary and a decrease ($P \leq 0.05$) in the epithelial height, luminal, and tubular diameters of seminiferous tubules at the two higher dosages. In addition, IMI had a negative effect on the immunostaining intensity of desmin, smooth muscle actin, and vimentin in the ovarian and testicular tissue. In conclusion, exposure to IMI during puberty can lead to a range of histopathological alterations in the gonads of Japanese quails, which may ultimately result in infertility.

1. Introduction

Neonicotinoid insecticides have been widely used to control agricultural pests and ectoparasites (Goulson, 2013). Despite their higher selectivity to nicotinic acetylcholine receptors of insects, as opposed to vertebrates (Shimomura et al., 2006), these insecticides can be easily released into the environment and accumulate in the soil, sediments, as well as surface and groundwater, which induces toxicity to non-target organisms (Hallmann et al., 2014). Exposure to neonicotinoids occurs by various means, such as consuming contaminated fruits, vegetables, and coated seeds, drinking surface water, and inhaling contaminated pollen (Zhang et al., 2018). Previous studies confirmed that exposure to neonicotinoids induces structural and functional changes in the male and female reproductive systems of fish, birds, and mammals, with the gonads being the main target (Akbulut, 2021; Eissa, 2004; Ibrahim et al.,

2020; Kenfack et al., 2018; Kong et al., 2017; Tokumoto et al., 2013; Zhao et al., 2021).

Among the numerous neonicotinoid compounds, imidacloprid [1-(6-chloro-3-pyridylmethyl)-N-nitroimidazolidin-2-ylideneamine] (IMI) is commonly utilized for controlling insects (Ensley, 2018; Tomizawa and Casida, 2005), but exposure to IMI causes adverse- and toxic effects in non-target organisms (Talpur et al., 2023). Although IMI is classified as a moderately toxic substance to mammals (class II by WHO and toxicity category II EPAV), there has been evidence of its reproductive toxicity and endocrine-disrupting properties (Kobir et al., 2023; Mikolić and Karačonji, 2018; Moreira et al., 2022; Mourikes et al., 2023; Zhao et al., 2021). Alterations in serum concentrations of follicle-stimulating (FSH) and luteinizing (LH) hormones were reported in female rats following treatment with 20 mg IMI/kg body weight (bw) for 90 days (Kapoor et al., 2011). Similarly, a decrease in testosterone concentration has

---

Table 1
Antibodies used for immunohistochemistry in this study.

Antibody (clone)	Dilution	Manufacturer
Desmin (monoclonal mouse ab6322)	1:300	Abcam, Cambridge, United Kingdom
Alpha-smooth muscle actin (monoclonal mouse 1A4)	1:50	DakoCytomation, Glostrup, Denmark
Vimentin (monoclonal mouse 3B4)	1:250	DakoCytomation, Glostrup, Denmark

been observed in adult male rats after exposure to 8 mg IMI/kg for 90 days (Bal et al., 2012a; Bal et al., 2012b). Pathomorphological changes in ovarian follicles and an increase in atretic follicles in adult rats exposed to 20 mg IMI/kg have been reported (Kapoor et al., 2011; Vohra and Khera, 2016). In addition, alterations in the testicular architecture, including disorganisation and detachment of the spermatogenic cells, as well as vacuolization in the seminiferous tubular epithelium in adult, male rats following exposure to 5.7 and 90 mg IMI/kg have been observed (Al-Awar, 2021; Sevim et al., 2023). Thus, IMI appears to be a reproductive toxicant in rats, but to our knowledge, little information is available on its effects on the gonads of birds, despite several toxicity incidents that have been reported in various avian species as a consequence of this compound (Botha et al., 2018; Millot et al., 2017; Rogers et al., 2019).

Reported sub-lethal effects resulting from IMI exposure in birds include a decrease in the total number of eggs and delay in the first egg lay date in adult female partridges (Lopez-Antia et al., 2015), oxidative stress and morphological alterations in the brain and liver of rock pigeons (Abu Zeid et al., 2019), and disruption of thyroid homeostasis and reproduction in wild birds (Pandey and Mohanty, 2015). Furthermore, there were morphological and inflammatory changes, oxidative stress, and fibrosis of the liver of Japanese quail following treatment with IMI at 2, 4, and 8 mg/kg (Lv et al., 2020). The decline of bird numbers across many species and ecosystems around the world has been attributed to the destruction of their natural habitats for agricultural purposes and the extensive use of insecticides, including IMI (Mitra et al., 2011; Suliman et al., 2020). Among bird species, the Japanese quail (*Coturnix coturnix*

japonica) is considered a sentinel species, foraging in agricultural lands, grass steppes, mountain slopes near water, and along riversides (Baer et al., 2015), making it susceptible to exposure to neonicotinoids. Therefore, the objective of the present study was to investigate the effect of imidacloprid (IMI) on the structure of the ovary and testis of Japanese quail that were exposed during puberty.

2. Materials and methods

2.1. Ethics statement

The study was approved by the University of Pretoria's Animal Ethics Committee (approval number 003–23), and animal health approval from the National Department of Agriculture, Land Reform, and Rural Development (DALRRD), South Africa (12/11/1/1/5 (2860ZY)). The experiment was conducted following the suggested guidelines for avian toxicity testing as stipulated by the Organization for Economic Co-operation and Development (OECD, 2022), with minor modifications. In addition, the Animal Research Reporting of *In Vivo* Experiments (ARRIVE) guidelines (Percie du Sert et al., 2020), the UK Animals (Scientific Procedures) Act, 1986 and associated guidelines, and EU Directive 2010/63/EU for animal experiments were followed in this study.

2.2. Chemicals

The test compound, imidacloprid [1-(6-chloro-3-pyridylmethyl)-N-nitroimidazolidin-2-ylideneamine] (IMI) used in this study was purchased from Sigma-Aldrich (Pty) Ltd (Johannesburg, South Africa). Imidacloprid was dissolved in distilled water at a concentration of 0.62 mg/ml for the high dose (6.2 mg/kg) and further serially diluted in distilled water to 0.31 and 0.155 mg/ml for both the medium (3.1 mg/kg) and low (1.55 mg/kg) doses, respectively.

2.3. Animals and management

A total of 28 female and male Japanese quail (*Coturnix coturnix*
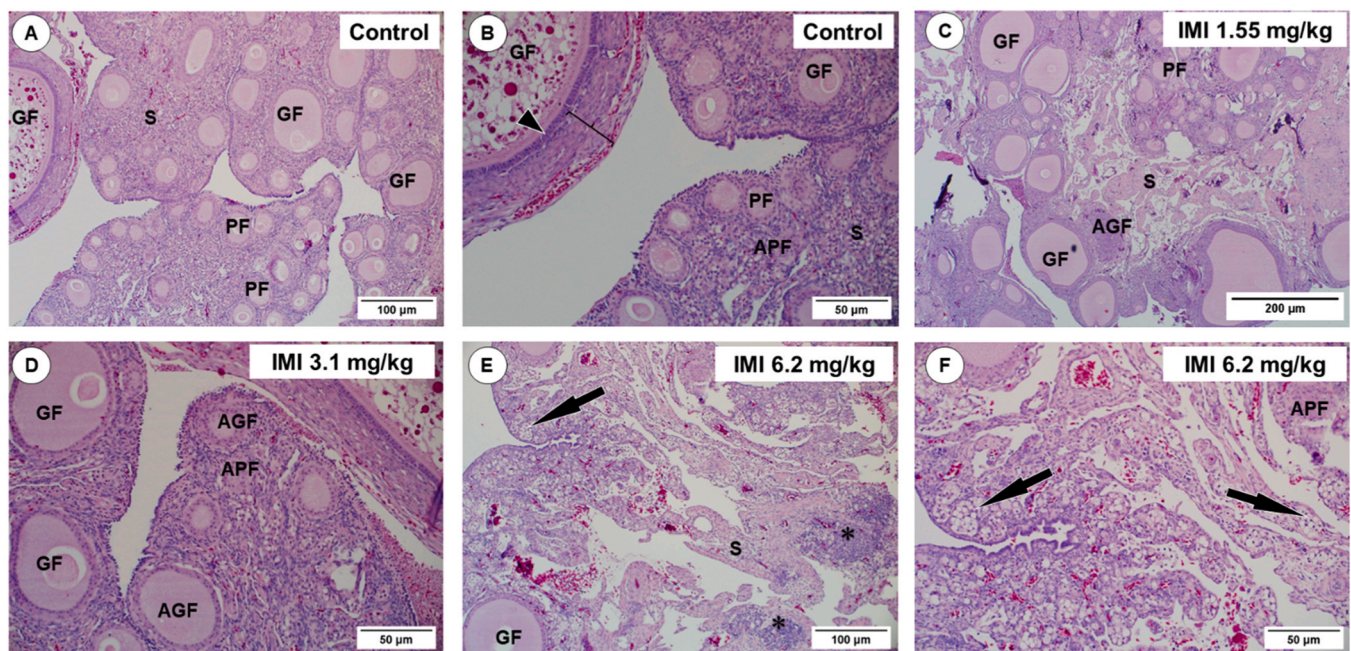
Fig. 1. Photomicrograph of the ovary of Japanese quails. (A & B) control, (C) 1.55, (D) 3.1 and (E & F) 6.2 mg IMI/kg. PF: Primary follicle. GF: Growing follicle. APF: Atretic primary follicle. AGF: Atretic growing follicle. S: Stroma. (B) Arrowhead: Granulosa cells. Bracket: Theca layer. (E) Asterisks: Lymphocyte infiltration in the stroma. (E & F) Arrows: Degenerated primary follicles.
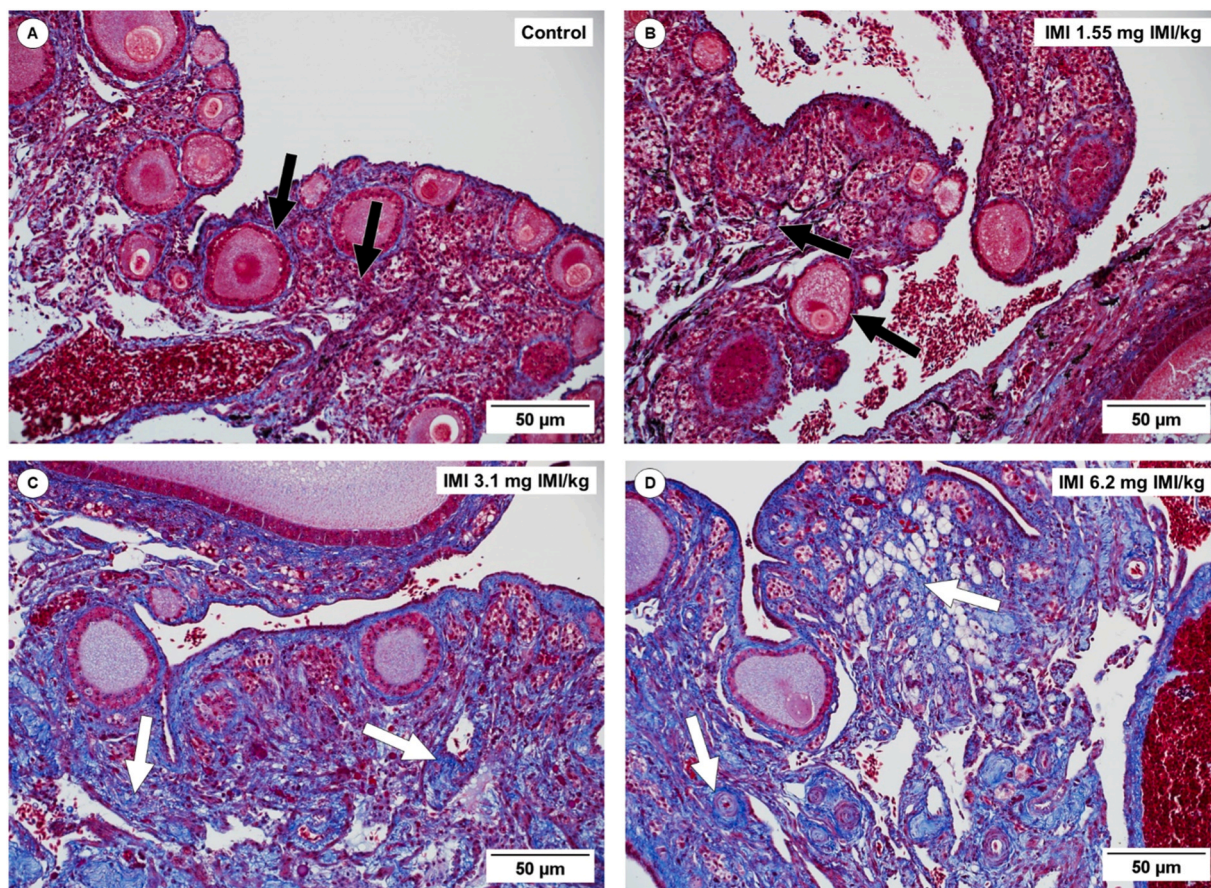
Fig. 2. Photomicrograph of Masson's trichrome staining of the ovary of Japanese quails. (A) control, (B) 1.55, (C) 3.1 and (D) 6.2 mg IMI/kg. Normal (black arrows) and dense (white arrows) deposition of collagen fibres in the follicular capsule and stroma of the ovaries.

japonica), at 3-week-old, were obtained from Zelda Enslin Farm, Pretoria, Gauteng Province, South Africa. Upon arrival, body weights were recorded (Jadever JWQ weighing scale; Fujian, China), and birds were kept for two weeks for acclimatization. The birds were fed a commercial standard diet (Alzu Voere Feeds, Pretoria, South Africa) and potable water were provided *ad libitum* throughout the experiment, and the daily feed intake was recorded. Birds were maintained under a controlled photoperiod (12 h light: 12 h dark) and temperature ($25 \pm 2\,^{\circ}$C) with a relative humidity of 50 ± 5 % in a room with a cement floor, which was covered with a layer of wood shavings, which was later divided into four separate pens of equal surface areas, for each group. The birds were housed at the Onderstepoort Veterinary Animal Research Unit (OVARU), University of Pretoria, South Africa. Throughout the experimental period, the birds were weighed once a week, and the IMI dose was adjusted accordingly. The birds were observed continuously during the first 2 h after dosing for regurgitation and the onset of clinical signs on at least three evenly spaced additional occasions during the day. Furthermore, to minimize the stress of weighing, the animals were weighed every second day from the day of dosing; if an animal were to lose more than 10 % of its body weight, since the previous weighing, it would have been euthanized.

2.4. Experimental design and dosing regimen

At the beginning of the experiments, quails were randomly divided into four groups at 5 weeks of age ($n = 7$ per group), with 4 females and 3 males in each group and were individually identified by wing tags. Birds were orally gavaged, twice per week for four weeks, as follows: Group 1 (control) was administered distilled water (a dose of 10 ml/kg). Groups 2, 3, and 4 (treatment) were dosed orally with 1.55, 3.1, and

6.2 mg/kg of imidacloprid dissolved in distilled water which represents 1/20, 1/10, and 1/5 of the LD_{50} (LD_{50} 31 mg/kg), respectively (SERA, 2005; EFSA, 2014), and were considered to be environmentally realistic exposure concentrations (Mineau and Palmer, 2013). The middle dose group of 3.1 mg/kg/d (10 percent of the LD_{50}) was selected based on the No-Observed-Adverse-Effect-Level (NOAEL) as determined in previous studies in Japanese quail (reviewed in Posthuma-Doodeman, 2008, SERA, 2005).

2.5. Sample collection

After 4 weeks of the dosing period, the birds were housed for an additional week to reach sexual maturity and euthanized by a gas mixture of 35 % CO_2, 35 % N_2, and 30 % O_2. Ovarian and testicular tissues were collected and immediately fixed in 10 % buffered formalin for at least 3 days for light microscopy or in 2.5 % glutaraldehyde in 0.075 M sodium phosphate buffer (pH 7.4) for at least 24 h for transmission electron microscopy (TEM). For the ovary, a small piece of ovarian tissue from each group was randomly selected, cut (~1 mm 3 blocks), and processed for TEM analysis.

2.6. Light microscopy

After fixation, ovaries and testes from both control and treatment groups were routinely processed for histology using an automated tissue processor (Shandon Excelsior Thermo Scientific, Germany), sectioned at 5 µm thick, and stained with hematoxylin and eosin (H&E) using a Shandon Vari-stainer (VHLSOP418; Thermo Electron Corp., Warwickshire, UK), and with Masson's trichrome (Bancroft and Gamble, 2008).
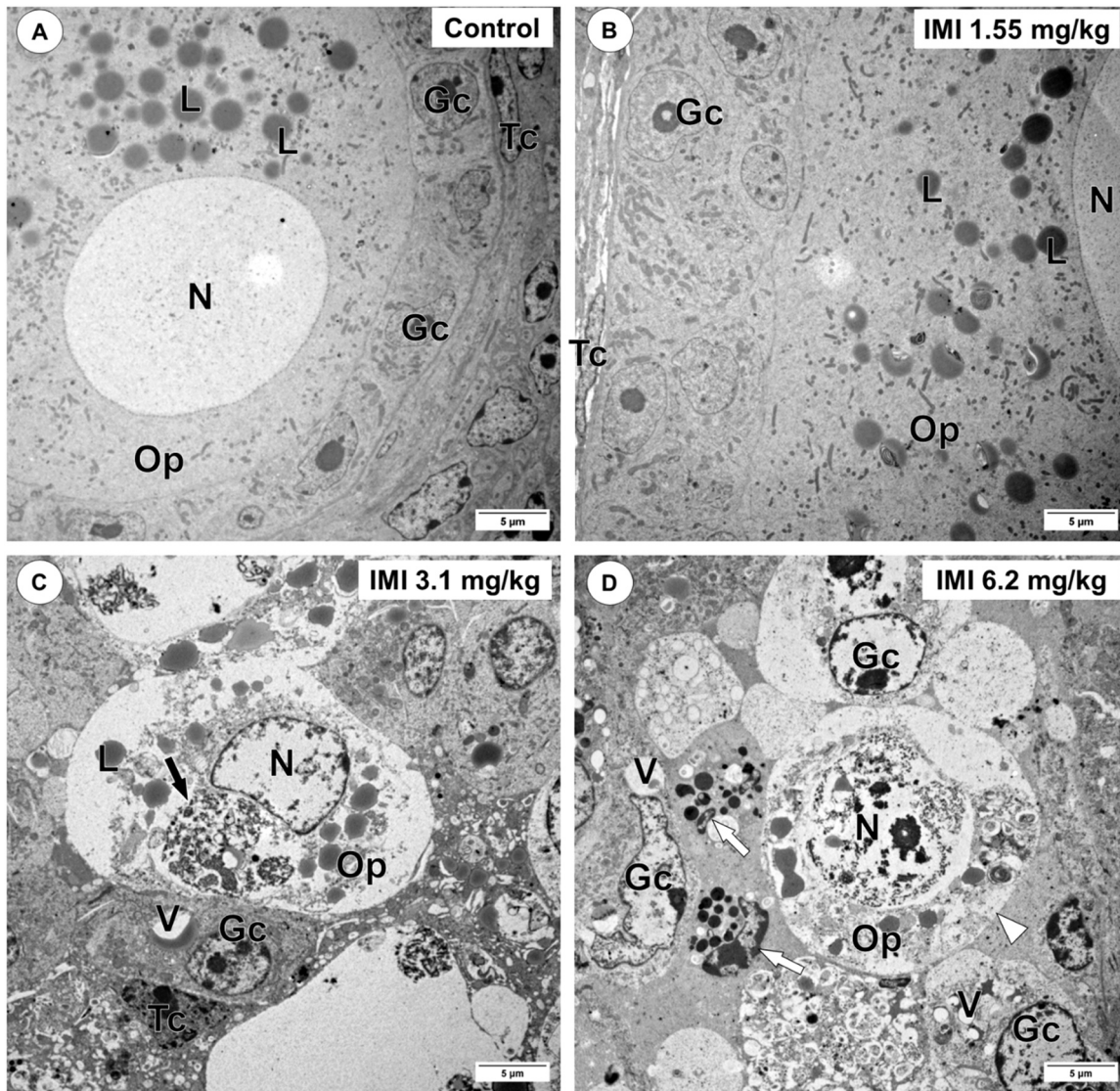
Fig. 3. Electron micrograph of the primary follicles of the ovary of Japanese quails. (A) control, (B) 1.55 mg IMI/kg, (C) 3.1, and (D) 6.2 mg IMI/kg. (A & B) Primary follicles with normal granulosa cells (Gc), theca cells (Tc), and ooplasm (Op) containing lipid droplets (L). (C & D) Degenerative cytoplasmic organelles (black arrow) in the ooplasm and cytoplasmic vacuoles (V) in the granulosa cells. (D) Necrosis of the oocyte (white arrowhead), and granulocyte infiltration (white arrows). N: Nucleus.

2.6.1. Histometric measurements

The measurements (in μm) of the testicular seminiferous tubules including epithelial heights, luminal and tubular diameters and cross-sectional area were performed using hematoxylin and eosin-stained sections at 20x magnification under light microscopy. All histometric measurements were carried out with Fiji-ImageJ software (Schindelin et al., 2012) in 5 rounded or nearly rounded seminiferous tubule cross-sections that were selected from at least 4 random microscopic fields per bird for each group. In addition, the number of primary and growing follicles, as well as atretic primary and growing follicles in 4 randomly selected microscopic fields per bird per group were counted. The ovarian follicles were classified based on the morphological structure described by Nad et al. (2007).

2.6.2. Immunohistochemistry

Tissue samples were cut at 3 μm sections, deparaffinized, rehydrated, and the endogenous peroxidase activity was blocked using 3 % (v/v) H_2O_2. For antigen retrieval, sections were microwaved at 750 W for 21 min in citrate buffer (pH 6). Thereafter, sections were incubated with specific primary antibodies, including alpha-smooth muscle actin

(SMA), desmin, and vimentin (Table 1), in a humidified chamber at 37 °C for 1 h. Subsequently, the sections were rinsed twice in phosphate-buffered saline solution (PBS) for 5 min each and then incubated in a humidified chamber at 37 °C with peroxidase-conjugated polymer of the DAKO Real Envision-HRP rabbit/mouse kit (DAKO EnVision™+ System, Peroxidase K5007, DAKO, Copenhagen, Denmark) for 15 min and then washed twice in PBS. Reactivity was visualized by applying a 3,30-dia-minobenzidine solution (DAB+) kit (DAKO EnVision™+ System, Peroxidase K5007, DAKO, Copenhagen, Denmark). The sections were then counterstained (Mayer's hematoxylin), dehydrated, cleared, and mounted. The same process was used for the positive controls.

The evaluation of immunohistochemistry was performed based on the method described by Crowe and Yue (2019), a semiquantitative analysis based on the relative staining intensity of immunolabeling of alpha-smooth muscle actin, desmin, and vimentin in the ovarian and testicular tissues was determined using Fiji-ImageJ software (Schindelin et al., 2012).
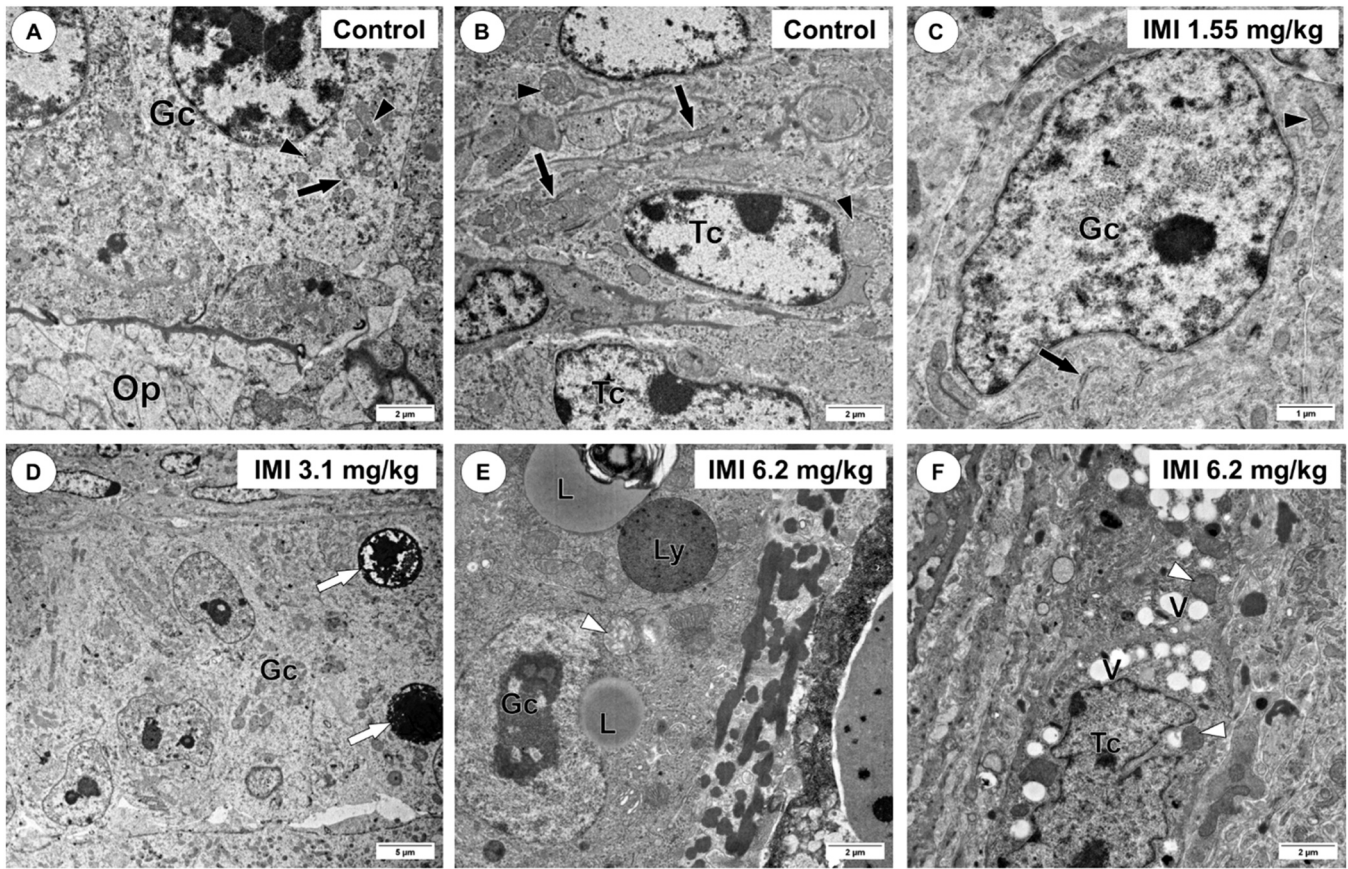
Fig. 4. Electron micrograph of the growing follicles of the ovary of Japanese quails. (A & B) control, (C) 1.55 mg IMI/kg, (D) 3.1, and (E & F) 6.2 mg IMI/kg. (A – C) Granulosa (Gc) and thecal (Tc) cells containing mitochondria (black arrowheads) and rough endoplasmic reticulum (black arrows). (D) Autophagosomes in the granulosa cells (white arrows). (E & F) large lipid droplets (L), and lysosome (Ly) in the cytoplasm of granulosa cells. White arrowheads indicate mitochondrial damage in the granulosa and thecal cells. (F) Cytoplasmic vacuoles (V) in the thecal cell. Op: Ooplasm
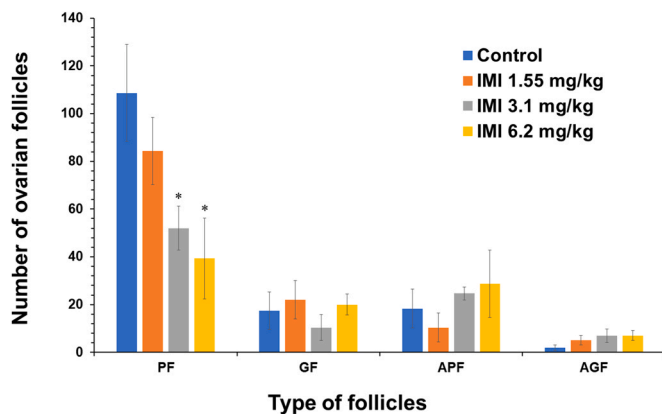
Fig. 5. The number (mean ± SE) of normal and atretic primary and growing follicles of the Japanese quail's ovary following twice weekly exposure to imidacloprid (IMI) at doses 1.55, 3.1, 6.2 mg/kg during puberty. A significant difference ($P \leq 0.05$) between the treatment groups (*) and the control group. PF: Primary follicle. GF: Growing follicle. APF: Atretic primary follicle. AGF: Atretic growing follicle.

2.7. Transmission electron microscopy

Following fixation, tissue samples were post-fixed in 1 % osmium tetroxide for 2 h. Thereafter, tissue samples were washed in 0.075 M sodium phosphate buffer, dehydrated in increasing alcohol concentrations, and embedded in epoxy resin 1:1 for 1 h, 1:1 for 2 h, and 100 % resin overnight. Then, ultra-thin sections (80–90 nm thick) were stained with uranyl acetate and counterstained with lead citrate. Images were acquired with a JEOL JEM 1400-FLASH transmission electron microscope (Tokyo, Japan).

2.8. Statistical analysis

The histometric measurements of the seminiferous tubules, the number of ovarian follicles, as well as semiquantitative analysis of alpha-smooth muscle actin (SMA), desmin, and vimentin were analyzed using IBM SPSS software version 28 (IBM Corp., Armonk, United States). Data were tested for normality by performing a homogeneity of variances test and plotting histograms and were analyzed using Tukey's Honest Significant Difference (HSD) post hoc, one-way analysis of variance (ANOVA) for comparisons between groups. Statistical significance was set at $P \leq 0.05$.

3. Results

3.1. Effect of imidacloprid on histomorphology, and histometry

3.1.1. Ovary

Histologically, in the control and 1.55 mg/kg IMI-treated groups, the ovarian tissue of the quail appeared normal and consisted of numerous primary and growing follicles at different stages of development (Fig. 1A–C). In addition, a few atretic primary and growing follicles were also detected. In quails treated with 3.1 and 6.2 mg IMI/kg, however, the ovarian structure showed atretic primary and growing follicles characterized by the overgrowth of the granulosa layer and loss of oocytes
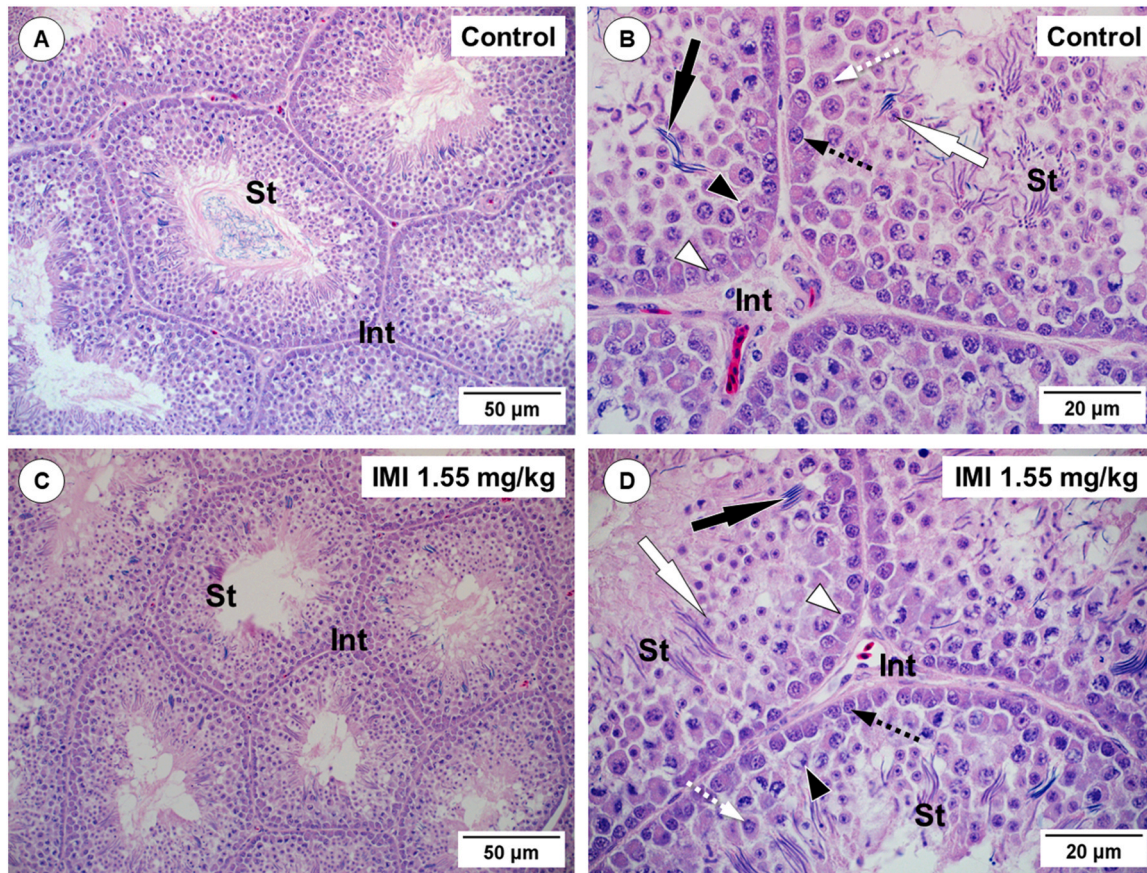
Fig. 6. Photomicrograph of seminiferous tubules of the testis of Japanese quails. (A & B) Control and (C & D) 1.55 mg IMI/kg. (A – D) Seminiferous tubules (St) exhibit normal and active germinal epithelium that contains Sertoli cells (black arrowheads), dark spermatogonia (dashed black arrows), pale spermatogonia (white arrowheads), spermatocyte (dashed white arrows), round spermatid (white arrows), and elongating spermatids (black arrows). Int: Interstitium.

(Fig. 1D, E). In addition, in quails treated with 6.2 mg IMI/kg, there were degenerated primary follicles associated with vacuolization and the accumulation of lymphocytes in the ovarian tissue (Fig. 1E, F). Masson's trichrome stain demonstrated presence of collagen fibres in the follicular capsule and stroma, but it was much denser in the birds treated with 3.1 and 6.2 mg IMI/kg, thus indicating fibrotic changes (Fig. 2 A–D).

Ultrastructurally, there were no differences in the primary and growing follicles of the quails treated with 1.55 mg IMI/kg and the control group (Figs. 3A, B and 4A–C). However, quails treated with 3.1 and 6.2 mg IMI/kg displayed marked changes in the primary and growing follicles. Necrosis in the oocyte, characterized by damage to the nuclear envelope and granulocyte infiltration, degenerative ooplasmic organelles, as well as cytoplasmic vacuoles in the granulosa cells of the primary follicles (Fig. 3C, D). In addition, there were large lipid droplets, mitochondrial damage, vacuoles, and lysosomes observed in the granulosa and thecal cells of growing follicles (Fig. 4D–F). Autophagosomes were also detected in the granulosa cells.

Histometrically, there was no difference in the number of growing follicles, and atretic primary and growing follicles of the ovary between quails treated with 1.55, 3.1 and 6.2 mg IMI/kg and control groups. In the quails treated with 3.1 and 6.2 mg IMI/kg, however, the number of primary follicles was significantly decreased ($P \leq 0.05$) compared to the control group (Fig. 5).

*3.1.2. Testis*

In the control quails, the seminiferous epithelium appeared morphologically normal, and they comprised typically arranged Sertoli cells, spermatogonia, spermatocytes, and round and elongated spermatids. Moreover, the testicular interstitium and its content including

Leydig cells appeared normal (Fig. 6A, B). There were no obvious morphological differences in the seminiferous tubule architecture in quails treated with 1.55 mg IMI/kg compared to those of the control group (Fig. 6C, D). In the groups treated with 3.1 and 6.2 mg IMI/kg, however, the architecture of seminiferous tubules appeared to be distorted, which was evident by the sloughed spermatogenic cells into the lumen, vacuolization in spermatogonia and Sertoli cells and reduction of elongated spermatids (Fig. 7A–D). Positive Masson's trichrome staining was observed in the peritubular tissue and interstitium of seminiferous tubules, but it was slightly denser in the birds treated with 3.1 and 6.2 mg IMI/kg, indicating deposition of collagen fibers (Fig. 8A–D).

Ultrastructurally, the control birds had normal seminiferous epithelium architecture, including intact nuclear membranes of spermatogonia, spermatocytes, and round and elongated spermatids (Fig. 9A–C). Seminiferous tubules of quail treated with 1.55 mg IMI/kg had noticeable nuclear membrane disruption of spermatogonia and cytoplasmic vacuoles in the peritubular myoid cells in comparison with the control group (Fig. 9D). However, the seminiferous tubules of quail treated with 3.1 and 6.2 mg IMI/kg showed marked ultrastructural changes, including the presence of cytoplasmic vacuoles in the spermatogonia and spermatocytes, as well as Sertoli cell degeneration with cytoplasmic vacuoles, shrinkage of the nucleus, and apoptotic body (Fig. 10A–D). Furthermore, Sertoli cells showed autophagosomes and mitochondrial damage (Fig. 10E, F).

Histometrically, there was no significant difference in the mean of epithelial height, luminal diameter, and tubular diameter of seminiferous tubules of the testis between quails treated with 1.55 mg IMI/kg and the control group (Table 2). In the quails dosed with 3.1 and 6.2 mg IMI/kg, however, the seminiferous epithelial height as well as the luminal
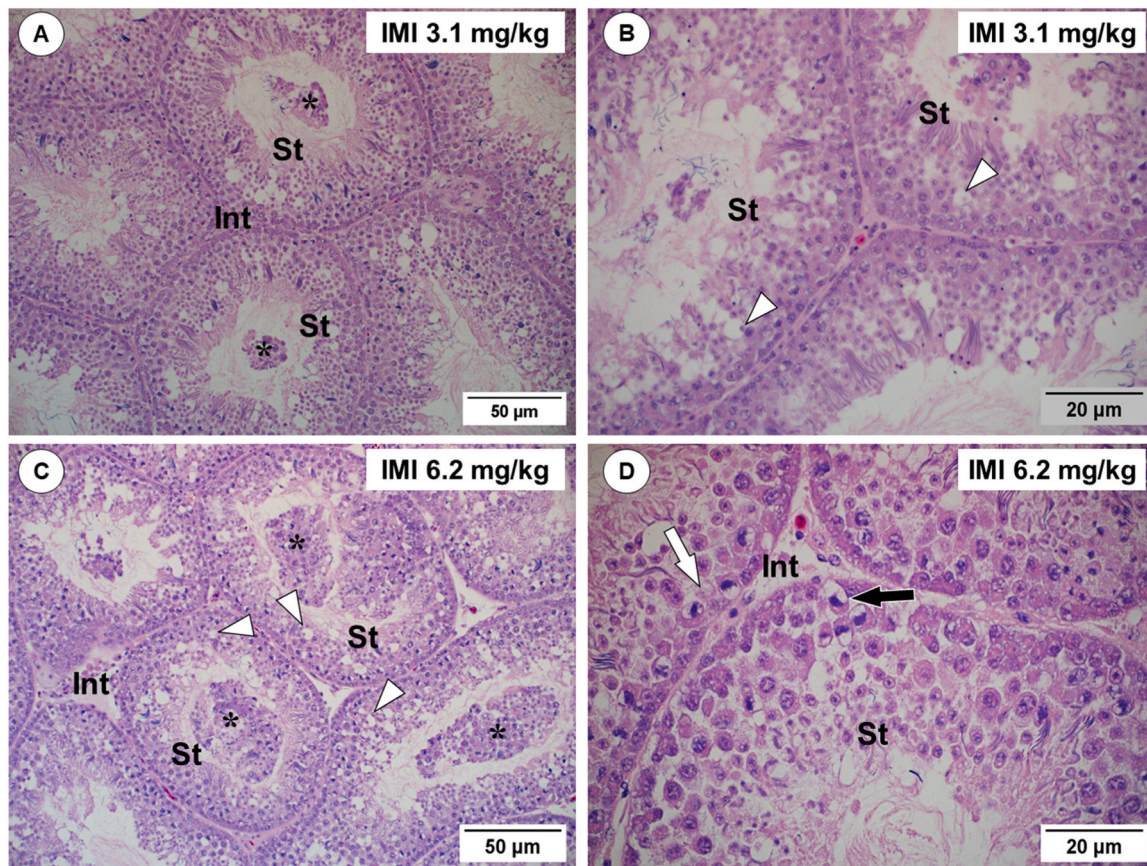
Fig. 7. Photomicrograph of seminiferous tubules (St) of the testis of Japanese quails exposed to (A & B) 3.1 and (C & D) 6.2 mg IMI/kg. (A & C) Asterisks indicate clumps of sloughed germinal cells in the lumen of seminiferous tubules. (B & C) White arrowheads show numerous vacuoles in the seminiferous epithelium. (D) Cytoplasmic vacuoles in the Sertoli cell (white arrow) and spermatogonium (black arrow). Int: Interstitium.

and tubular diameter of the seminiferous tubules were significantly reduced ($P \leq 0.05$) when compared to the control group (Table 2). In addition, the cross-sectional area of seminiferous tubules was significantly decreased ($P \leq 0.05$) in all treatments compared to those in the control group (Table 2).

3.2. Effect of imidacloprid on the structure of desmin, smooth muscle actin and vimentin

3.2.1. Ovary

There were no obvious differences in the immunolabeling or distribution of desmin, SMA, and vimentin in the ovarian tissue of all treated groups compared to those of the control group (Fig. 11A–C). Desmin and SMA immunolabeling were observed in stromal cells, the muscular layer of blood vessels, as well as surrounding regions in primary and growing follicles (Fig. 11A, B). Vimentin was immunopositive in granulosa cells of both primary and growing follicles and stromal cells (Fig. 9C). Furthermore, the semiquantitative analysis revealed that the integrated intensity of desmin and SMA immunostaining in the ovarian tissue in all IMI-treated groups was lower ($P \leq 0.05$) compared to the birds in the control group, while the integrated intensity of vimentin in the birds treated with 3.1 and 6.2 mg IMI/kg was less ($P \leq 0.05$) compared to the control group (Fig. 11D).

3.2.2. Testis

The peritubular tissue in the control and all IMI-treated birds was immunopositive for desmin, SMA, and vimentin (Fig. 12A–C). However, the semiquantitative analysis revealed that the integrated intensity of desmin immunostaining in the peritubular tissue in the quails treated with 3.1 and 6.2 mg IMI/kg was higher ($P \leq 0.05$) compared to the birds

in the control group, while the integrated intensity of SMA in all IMI-treated birds was lower ($P \leq 0.05$) compared to the control group (Fig. 12D). However, the integrated intensity of vimentin was significantly increased ($P \leq 0.05$) in the group treated with 1.55 IMI/kg and decreased ($P \leq 0.05$) in the group treated with 3.1 and 6.2 mg IMI/kg (Fig. 12D).

4. Discussion

Among neonicotinoid insecticides, imidacloprid (IMI) is one of the most commonly detected environmental contaminants (Wang et al., 2022). Mammals and birds are exposed to IMI via several routes and consequently, it enters their bodily fluids (Zhao et al., 2020), and may induce toxicity. Imidacloprid and its metabolites have been detected in the testis of mice (Nimako et al., 2021), as well as the ovary of rats (Kapoor et al., 2014). In the current study, IMI induced several histopathological and ultrastructural changes in the ovary and testicular tissue of Japanese quail (*Coturnix coturnix japonica*) when exposed during puberty. More distinct lesions were observed in the quails treated with 3.1 and 6.2 mg IMI/kg, twice per week for 4 weeks, than birds treated with 1.55 mg IMI/kg and the control birds.

4.1. Effect of imidacloprid on ovary

Since the ovary fulfills the essential role of developing and releasing oocytes as well as the synthesis of various steroid hormones (Onagbesan et al., 2009), any toxic agent that causes injury to the ovary might lead to abnormal follicle formation (He et al., 2020; Qin et al., 2015). Results of the current study indicated that IMI induced dose-dependent negative effects on the ovarian structure of the Japanese quail. In rats the
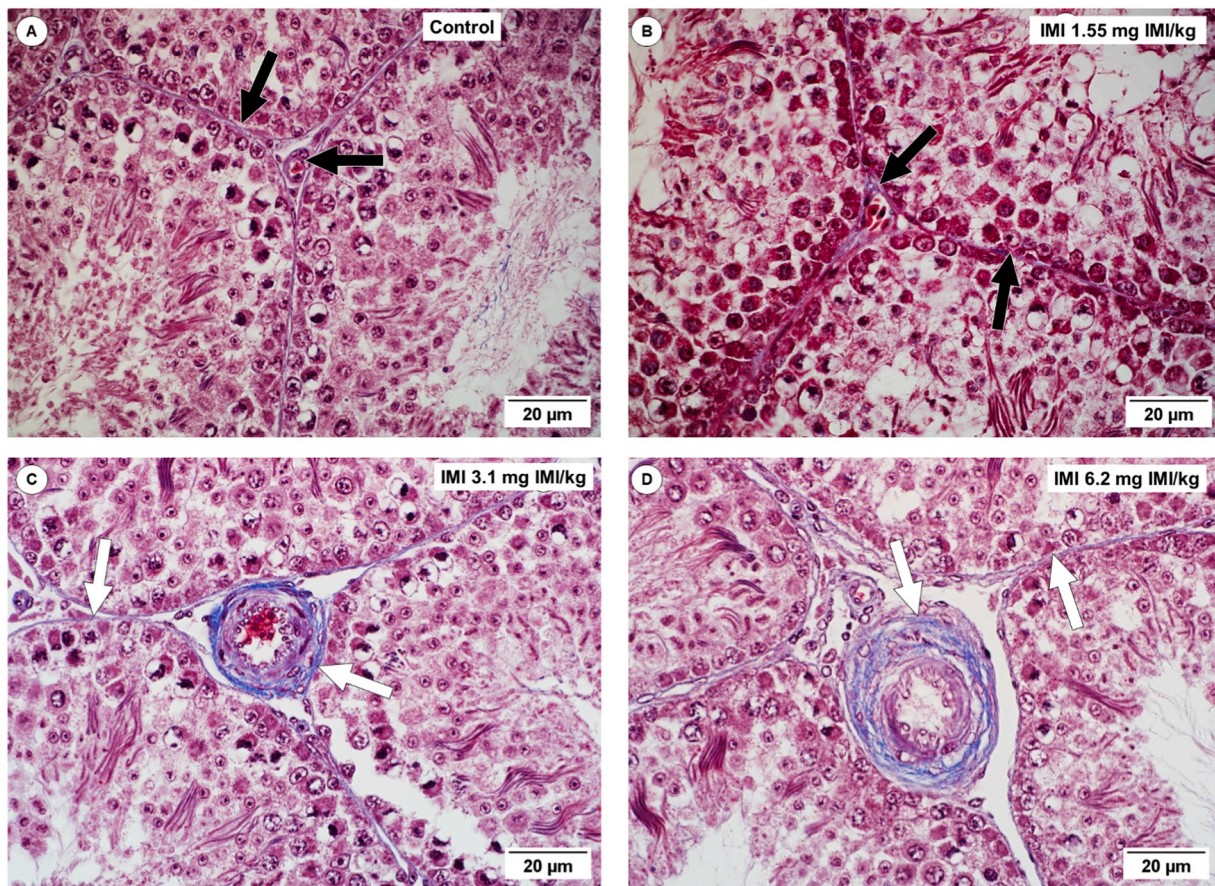
Fig. 8. Photomicrograph of Masson's trichrome staining of the testis of Japanese quails. (A) control, (B) 1.55, (C) 3.1 and (D) 6.2 mg IMI/kg. Normal (black arrows) and dense (white arrows) deposition of collagen fibres in the interstitium and peritubular tissue of the seminiferous tubules.

administration of IMI causes histopathological disruptions in the ovary by decreasing the number of healthy follicles (Nabiuni et al., 2015; Sood, 2023). Imidacloprid also induces oocyte degeneration and cytoplasmic clumping of the granulosa cells in rats (Kapoor et al., 2011; Lohiya et al., 2019). The current study demonstrated that IMI at doses of 1.55, 3.1, and 6.2 mg/kg twice per week for 4 weeks induced a significant decrease in the number of primary follicles. Furthermore, the quails treated with 3.1 and 6.2 mg IMI/kg showed degenerative changes, including lymphocyte accumulation in the ovarian stroma (Fig. 1E, F), necrosis associated with damage to the nuclear envelope, and granulocyte infiltration in the ovarian follicular cells (Fig. 3D). Imidacloprid has been reported to induce oxidative stress in the ovarian tissue of rats (Kapoor et al., 2011; Lohiya et al., 2019; Mzid et al., 2018), and studies have demonstrated that oxidative stress in the ovaries adversely affects oocyte quality (Prasad et al., 2016), triggers apoptosis in granulosa cells (Sohel et al., 2019), which suggested that the morphological changes in the quail ovary could be attributed to the stimulation of oxidative stress mechanisms by IMI.

The cytoskeletal proteins, including desmin and vimentin intermediate filaments and smooth muscle actin (SMA) microfilaments, are involved in cellular communications, morphology, maintenance, and support (Jimenez-Lopez, 2017). Desmin, vimentin and SMA are present in the follicular and stromal cells of ovaries in experimental birds, mammals, and reptiles (da Silveira Firmiano et al., 2021; Madekurozwa, 2007; Marettová and Maretta, 2002; Rodler et al., 2015; Van Nassauw and Callebaut, 1991). In the current study, no obvious differences were seen in the distribution of desmin, SMA, and vimentin in the ovaries of all treated groups compared to the control group, however, the immunolabeling intensity of desmin and SMA in the ovarian tissue in all IMI-treated groups was lower ($P \leq 0.05$) compared to the birds in the

control group. In addition, the integrated intensity of vimentin immunostaining in the birds treated with 3.1 and 6.2 mg IMI/kg was less ($P \leq 0.05$) compared to the control group (Fig. 11D). da Silveira Firmiano et al. (2021) suggested that desmin and SMA play a role in the development of follicles and ovulation through their contractile activities. Vimentin is also involved in various aspects of granulosa cell activity, atresia, and intercellular transport (Van den Hurk et al., 1995). Thus, it is probable that the effect on the cytoskeletal filaments observed in this study could contribute to reduced fertility in female quail following exposure to IMI during puberty.

4.2. Effect of imidacloprid on testis

The division, differentiation, and migration of germ cells, from the basal lamina to the tubular lumen, occurs within the seminiferous tubules of the testis (Deviche et al., 2011). In the present study, the quail treated with 3.1 and 6.2 mg IMI/kg had more histopathological abnormalities in the seminiferous tubules when compared with the control birds. There was a distortion in the architecture of the seminiferous tubules associated with the sloughing of spermatogenic cells into the lumen, vacuole formation in spermatogonia and Sertoli cells, and reduced elongated spermatids (Fig. 7B–D). In addition, the current study also revealed that there was a significant decrease ($P \leq 0.05$) in the epithelial height and the luminal and tubular diameter of the seminiferous tubules in the birds exposed to 3.1 and 6.2 mg IMI/kg (Table 1). The results of the current study is in agreement with the findings reported by Eissa (2004) who described vacuolation in the spermatocytes, the disappearance of spermatogenetic cells, pyknotic changes, and a reduction in sperm within the seminiferous tubules of Japanese quail exposed to IMI. A decrease in epithelial height and diameter of
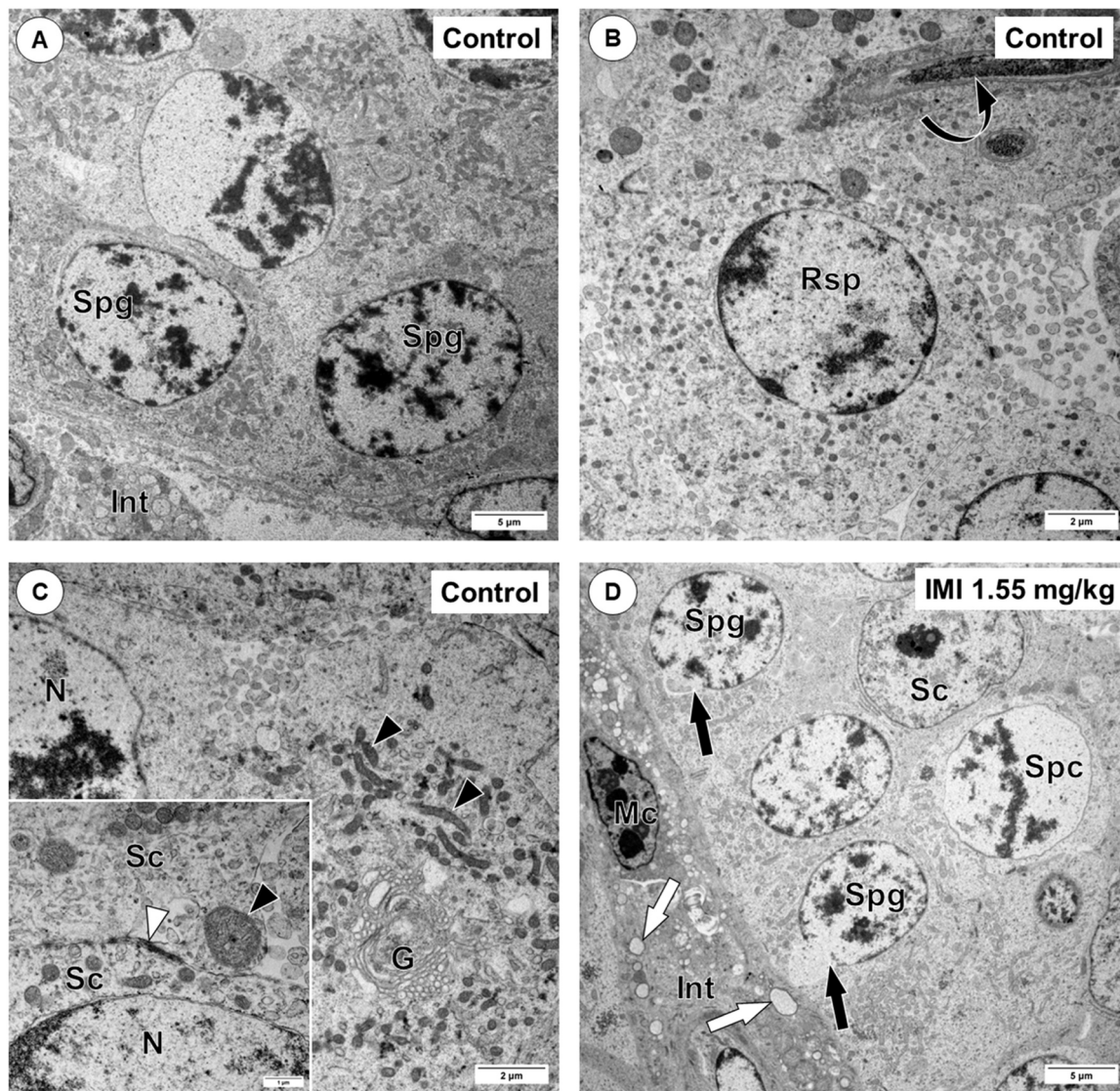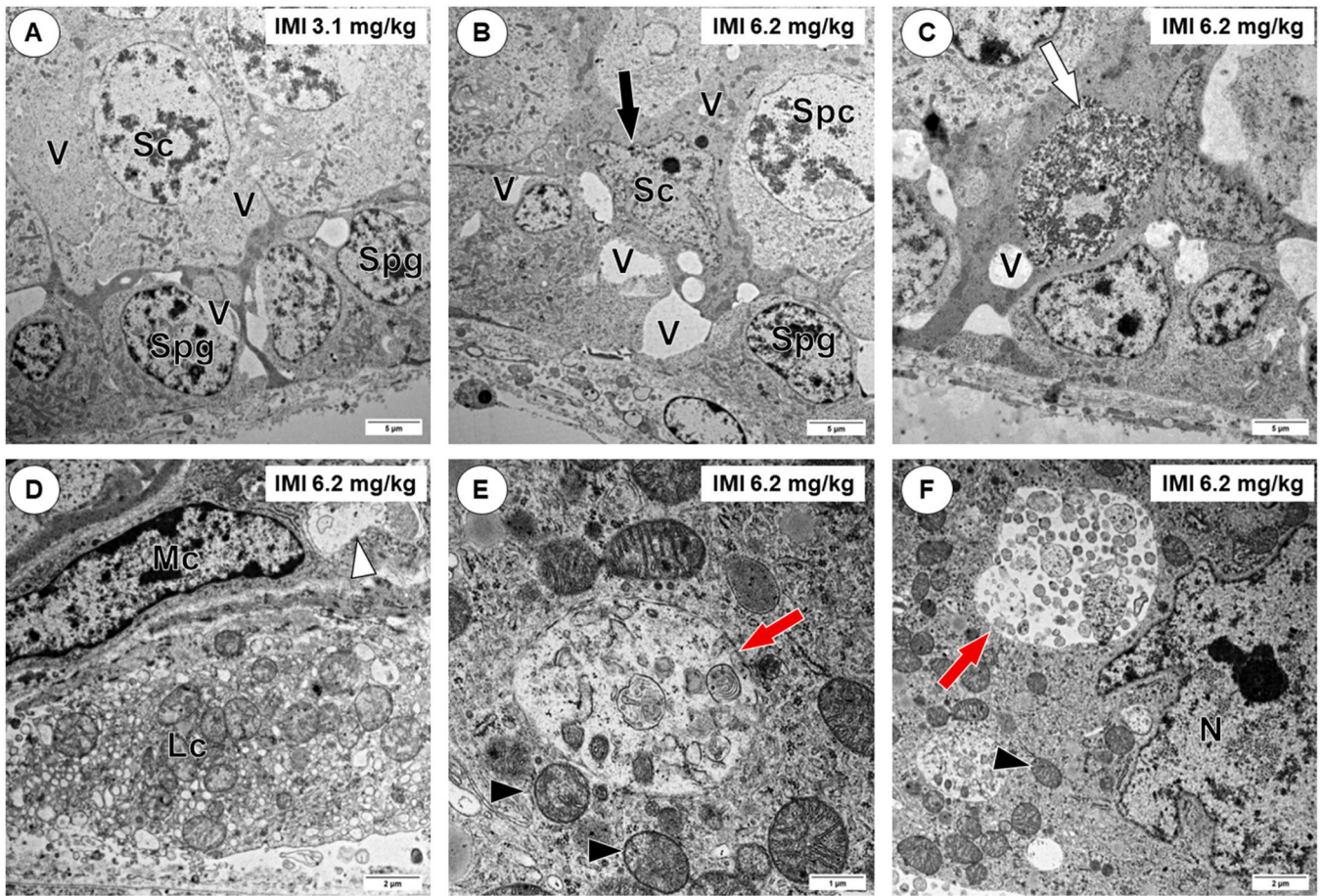
Fig. 9. Electron micrograph of seminiferous tubules of the testis of Japanese quails. (A – C) Control and (D) 1.55 mg IMI/kg. Spg Spermatogonia. Spc: Spermatocyte. Rsp: Round spermatid. Sc: Sertoli cell. Int: Interstitium. Mc: Myoid cell. N: Nucleus. G: Golgi complex. (B) Elongated spermatid (curved arrow). (C) Black arrowheads: Mitochondria. Inset: Adherent junctions (white arrowhead) between adjacent Sertoli cells. (D) Disruption of the nuclear membrane of spermatogonia (black arrows) and cytoplasmic vacuoles within myoid cell (white arrows).

seminiferous tubules and a reduction in Leydig cell density are also reported in the testis of red munia after exposure to IMI (Mohanty et al., 2017). Spermatogenesis in the seminiferous tubules is regulated by steroid hormones (Johnson et al., 2000). Imidacloprid disrupts the synthesis of steroid hormones by impairing the activity of the cytochrome P450 (CYP) enzymes (Abdel-Razik et al., 2021; Bhaskar et al., 2014; Yang et al., 2020), and it is evidenced that hormonal imbalances can lead to disruptions in intercellular junctions between Sertoli and germ cells, leading to the sloughing of germ cells from the seminiferous tubule epithelium (Kolasa et al., 2011; Martinez et al., 2009). Therefore, oxidative stress or a hormonal imbalance caused by IMI could be responsible for the morphological changes in testicular seminiferous tubules of quail observed in this study.

In the current study, there was cytoplasmic vacuolization in germ and Sertoli cells in quails treated with 3.1 and 6.2 mg IMI/kg- (Fig. 10A–C). Sertoli cells also showed degenerative changes, including debris of apoptotic bodies, autophagosomes, and mitochondrial damage (Fig. 10E, F). Exposure to IMI induces apoptosis and necrosis in the interstitium, and apoptosis in Leydig cells of red munia (Mohanty et al., 2017). The degenerative changes in the seminiferous tubule epithelium

are suggestive of a morphological indication of IMI-associated testicular toxicity, whereby IMI induces toxicity by inducing oxidative stress (Bal et al., 2012a; Kobir et al., 2023; Yang et al., 2020). Previous studies concluded that IMI induces oxidative stress in the testicular tissue of rats (Keles et al., 2022; Mahajan et al., 2018; Saber et al., 2021), which resulted in severe degenerative changes in the seminiferous tubules including depletion of germ cells, necrosis, and tubular shrinkage (Mahajan et al., 2018).

Desmin, SMA and vimentin are present in the peritubular tissue of birds and play an important role in the expulsion of immobile spermatozoa into the excurrent duct system (Aire and Ozegbe, 2007; Madekurozwa, 2013; Ozegbe et al., 2008a). No obvious changes in immunolabeling or distribution of desmin, SMA, and vimentin in the peritubular tissue were observed in all groups exposed to IMI and the control group (Fig. 10A–C). The semiquantitative analysis, however, revealed a significant ($P \leq 0.05$) decrease in the integrated intensity of SMA in all IMI-treated birds compared to the control group ((Fig. 10D). The smooth muscle actin is an isoform of contractile actin that is present in the peritubular smooth muscle cells of the testis of birds and plays a crucial role in transporting testicular fluid and its cellular content into

Fig. 10. Electron micrograph of seminiferous tubules of the testis of Japanese quails exposed to (A) 3.1 and (B – F) 6.2 mg IMI/kg. (A – C) Small and large vacuoles (V) in the cytoplasm of spermatogonia (Spg), spermatocytes (Spc) and Sertoli cells (Sc). (B & C) Degenerate Sertoli cells are characterized by nuclear shrinkage (black arrow) and apoptotic body (white arrow). (D) Indicates large vacuole (white arrowhead) in the cytoplasm of myoid cell (Mc). (E & F) Depict autophagosomes (red arrows) and damaged mitochondria (black arrowheads) in the Sertoli cells. Lc: Leydig cell. N: Nucleus.

Table 2

The histometrical measurements (Mean $\pm$ SE) in the Japanese quail testes following exposure to imidacloprid (IMI) at doses 1.55, 3.1, 6.2 mg/kg twice per week during puberty.

Parameters (μm)	Control	IMI 1.55 mg/kg	IMI 3.1 mg/kg	IMI 6.2 mg/kg
SEH	139.7 $\pm$ 6.2	131.4 $\pm$ 2.1	108.3 $\pm$ 1.4[a]	95.3 $\pm$ 1.5[a]
SLD	274.8 $\pm$ 12.9	288.9 $\pm$ 8.9	232.7 $\pm$ 6.3[a]	228.3 $\pm$ 5.5[a]
STD	560.6 $\pm$ 18.9	482.8 $\pm$ 7.9	426.6 $\pm$ 13.9[a]	402.9 $\pm$ 8.0[a]
AST	267767.5 $\pm$ 7695.1	222167.5 $\pm$ 8434.9[a]	179307.5 $\pm$ 2766.4[a]	159287.5 $\pm$ 2859.4[a]

SEH: Seminiferous epithelial height. SLD: Seminiferous luminal diameter. STD: Seminiferous tubular diameter. AST: Area of seminiferous tubules.

[a] Denotes significant differences between treatments and control group ($P \leq 0.05$).

the excurrent duct (Ozegbe et al., 2008b). Therefore, the reduction in the SMA observed in this study could affect the contractile function of the testicular peritubular myoid cells.

In the current study, the vimentin intensity increased in the group treated with 1.55 mg IMI/kg and decreased in the groups treated with 3.1 and 6.2 mg IMI/kg (all $P \leq 0.05$). Similarly, Bao et al. (2011) reported an increase in vimentin expression at low doses and a decrease at higher doses in the testes of Sprague Dawley rats after exposure to di-n-butyl phthalate during puberty. The increase in vimentin expression might be ascribed to the hormetic response to a low dose of IMI (Lu et al., 2016). The collapse of vimentin intermediate filaments has been reported in a rat Leydig cell line (LC-540) after exposure to IMI (Ibrahim et al., 2023), as well as in Sertoli cells in the testis of rats after treatment with the organochlorine pesticide, 1,1-dichloro-2,2bis(p-chlorophenyl) ethylene (p,p′-DDE) (Yan et al., 2013). It has been reported that damage to vimentin intermediate filaments disintegrates seminiferous tubular epithelium (Kopecky et al., 2005), which is consistent with our observations where IMI induced morphological changes in the epithelium of the seminiferous tubules at doses of 3.1 and 6.2 mg IMI/kg.

Surprisingly, opposed to quail ovary results, there was a significant ($P \leq 0.05$) increase in the staining intensity of desmin observed in the peritubular tissue in the quails treated with 3.1 and 6.2 mg IMI/kg compared to the birds in the control group (Fig. 10D). There may be a gender difference in how the ovarian and testicular desmin filaments are affected by IMI, but further research is needed to explore this hypothesis. Desmin intermediate filaments are expressed in all myofiber networks and play an important role to resist mechanical and oxidative stresses (Costa et al., 2004). The aggregation of desmin has been linked to a variety of myopathies (Singh et al., 2020). Aggregation of desmin is considered a cellular protective response to acute injury, but it can also impair proteostasis and cause disease (Singh et al., 2020).

Furthermore, dense collagen fibre deposition was observed in the ovarian stroma of birds treated with 3.1 and 6.2 mg IMI/kg, compared to the control group. However, the collagen fibres were only slightly denser in the peritubular tissue and interstitium of seminiferous tubules in birds treated with 3.1 and 6.2 mg IMI/kg when compared to the control group. Inflammation, immune abnormalities, and oxidative
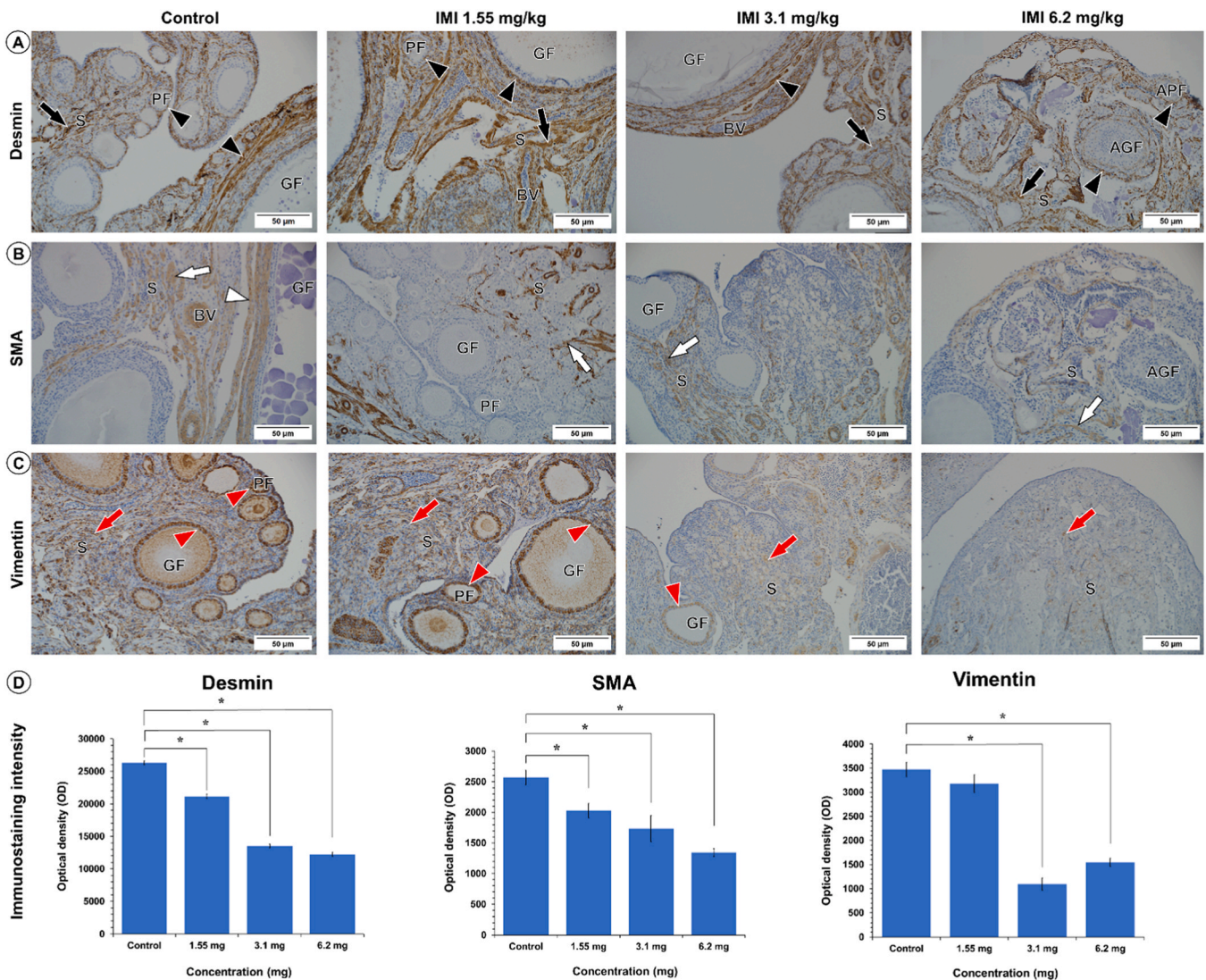
Fig. 11. Immunohistochemical staining of desmin, smooth muscle actin (SMA), and vimentin in the ovary of the Japanese quail after exposure to 1.55, 3.1, and 6.2 mg imidacloprid (IMI)/kg twice per week during puberty. (A) Black arrows indicate desmin immunopositive labeling in the stroma (S). The black arrowheads indicate regions of positive desmin immunostaining around primary (PF), growing (GF) and growing atretic (AGF) follicles. (B) Positive immunolabeling for SMA in the stroma (white arrows) and the area surrounding growing follicles (white arrowhead). (C) The red arrows indicate vimentin immunolabeling in the stroma. Immunopositive vimentin in the granulosa cells of primary (PF) and growing (GF) follicles are indicated by red arrowheads. APF: Atretic primary follicle. AGF: Atretic growing follicle. BV: Blood vessel. Bar = 50 μm. (D) Semiquantitative analysis of immunostaining intensity of desmin, SMA, and vimentin in ovarian tissue of the Japanese quails following treatment with 1.55, 3.1, and 6.2 mg IMI/kg. A significant difference ($P \leq 0.05$) between the treatment groups (*) and the control group. Data are presented as mean ± standard error (SE).

stress can cause ovarian fibrosis, hence increasing the susceptibility to infertility (Zhou et al., 2017). Imidacloprid and deltamethrin exposure induce liver fibrosis in Japanese quail, which are linked to inflammation and oxidative stress (Deng et al., 2022; Li et al., 2021). In this study, exposure to IMI induced an accumulation of lymphocytes in the ovarian tissue (Fig. 1E). Therefore, it is deduced that IMI may cause fibrosis in the ovary of quails via oxidative stress and inflammation. However, further studies are needed to investigate the mechanism of fibrosis in the ovary caused by IMI.

5. Conclusion

In conclusion, the current study demonstrated that pubertal exposure to imidacloprid doses of 1.55, 3.1 and 6.2 mg/kg, twice per week for 4 weeks, produces toxic effects on the gonads of the Japanese quail by inducing pathomorphological lesions and negatively affecting the cytoskeletal proteins in the ovary and testis in a dose-dependent manner.

Consequently, it appears that Japanese quail ovaries and testes may be susceptible to IMI-induced reproductive toxicity that could lead to infertility. More attention needs to be paid to the adverse and toxic effects of neonicotinoids in the environment.

Author agreement statement

All authors affirm that this manuscript is original, has not been published before and is not currently being considered for publication elsewhere. In addition, authors have confirmed that the manuscript has been read and approved by all named authors and that there are no other persons who satisfied the criteria for authorship but are not listed. Therefore, there is no conflict of interest.

Authors understand that the Corresponding Author is the sole contact for the Editorial process. He is responsible for communicating with the other authors about progress, submissions of revisions and final approval of proofs.
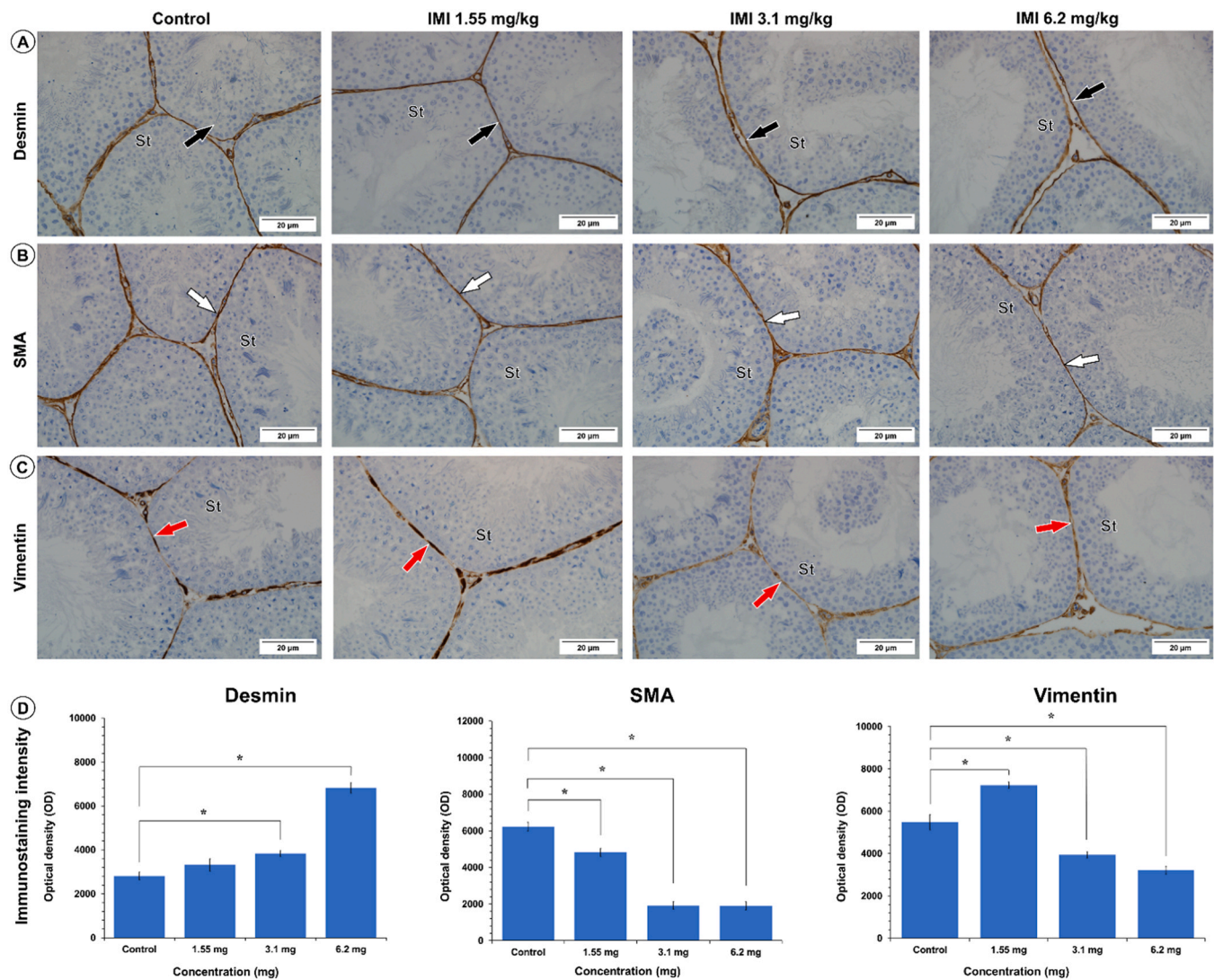
Fig. 12. Immunohistochemical staining of desmin, smooth muscle actin (SMA), and vimentin in the testis of the Japanese quail after exposure to 1.55, 3.1, and 6.2 mg imidacloprid (IMI)/kg twice weekly during puberty. (A – C) Immunopositive labeling of desmin (black arrows), SMA (white arrows) and vimentin (red arrows) in the peritubular tissue of the seminiferous tubules of the testis. St: Seminiferous tubule. Bar = 20 μm. (D) Semiquantitative analysis of immunostaining intensity of desmin, SMA, and vimentin in peritubular tissue in the testis of Japanese quails exposed to 1.55, 3.1, and 6.2 mg IMI/kg twice weekly during puberty. A significant difference ($P \leq 0.05$) between the treatment groups (*) and the control group. Data are presented as mean ± standard error (SE).

Declaration of Competing Interest

The authors declare that they have no competing financial interests or personal relationships that may have inappropriately influenced them in writing this article.

Data Availability

Data will be made available on request.

Acknowledgement

References

Abdel-Razik, R.K., Mosallam, E.M., Hamed, N.A., Badawy, M.E.I., Abo-El-Saad, M.M., 2021. Testicular deficiency associated with exposure to cypermethrin, imidacloprid, and chlorpyrifos in adult rats. Environ. Toxicol. Pharmacol. 87, 103724 https://doi.org/10.1016/j.etap.2021.103724.

Abu Zeid, E.H., Alam, R.T.M., Ali, S.A., Hendawi, M.Y., 2019. Dose-related impacts of imidacloprid oral intoxication on brain and liver of rock pigeon (*Columba livia domestica*), residues analysis in different organs. Ecotoxicol. Environ. Saf. 167, 60–68. https://doi.org/10.1016/j.ecoenv.2018.09.121.

Aire, T.A., Ozegbe, P., 2007. The testicular capsule and peritubular tissue of birds: Morphometry, histology, ultrastructure and immunohistochemistry. J. Anat. 210, 731–740. https://doi.org/10.1111/j.1469-7580.2007.00726.x.

Akbulut, C., 2021. Acute exposure to the neonicotinoid insecticide imidacloprid of zebrafish (*Danio rerio*) gonads: a histopathological approach. Int. J. Limnol. 57, 23. https://doi.org/10.1051/limn/2021021.

Al-Awar, M.S., 2021. Effect of imidacloprid on the testicular activity and endocrine disruptive and its impact on fertility in male rats. Indian J. Forensic Med. Toxicol. 15, 4695–4710.

Baer, J., Lansford, R., Cheng, K., 2015. Japanese quail as a laboratory animal model, in (Eds). In: Fox, J.G., Anderson, L.C., Otto, G.M., Pritchett-Corning, K.R., Whary, M.T. (Eds.), Laboratory animal medicine. Academic Press, Boston, pp. 1087–1108. https://doi.org/10.1016/B978-0-12-409527-4.00022-5 (Eds).

Bal, R., Naziroğlu, M., Türk, G., Yilmaz, Ö., Kuloğlu, T., Etem, E., Baydas, G., 2012a. Insecticide imidacloprid induces morphological and DNA damage through oxidative

toxicity on the reproductive organs of developing male rats. Cell Biochem. Funct. 30, 492–499. https://doi.org/10.1002/cbf.2826.

Bal, R., Türk, G., Tuzcu, M., Yilmaz, O., Kuloglu, T., Gundogdu, R., Gür, S., Agca, A., Ulas, M., Çambay, Z., 2012b. Assessment of imidacloprid toxicity on reproductive organ system of adult male rats. J. Environ. Sci. Health, Part B 47, 434–444. https://doi.org/10.1080/03601234.2012.663311.

Bancroft, J.D., Gamble, M., 2008. Theory and practice of histological techniques. Elsevier Health Sci.

Bao, A.M., Man, X.M., Guo, X.J., Dong, H.B., Wang, F.Q., Sun, H., Wang, Y.B., Zhou, Z. M., Sha, J.H., 2011. Effects of di-n-butyl phthalate on male rat reproduction following pubertal exposure. Asian J. Androl. 13, 702–709 https://doi.org/10.1038%2Faja.2011.76.

Bhaskar, R., Mishra, A.K., Mohanty, B., 2014. Effects of mancozeb and imidacloprid pesticides on activities of steroid biosynthetic enzymes cytochromes p450. J. Kalash Sci. 2, 1–6.

Botha, C.J., Du Plessis, E.C., Coetser, H., Rosemann, M., 2018. Analytical confirmation of imidacloprid poisoning in granivorous cape spurfowl (*pternistis capensis*). J. South Afr. Vet. Assoc. 89, 1–5 https://hdl.handle.net/10520/EJC-f98b9fc59.

Costa, M., Escaleira, R., Cataldo, A., Oliveira, F., Mermelstein, C., 2004. Desmin: Molecular interactions and putative functions of the muscle intermediate filament protein. Braz. J. Med. Biol. Res. 37, 1819–1830. https://doi.org/10.1590/S0100-879X2004001200007.

Crowe, A.R., Yue, W., 2019. Semi-quantitative determination of protein expression using immunohistochemistry staining and analysis: an integrated protocol. e3465-e3465 Bio-Protoc. 9. https://doi.org/10.21769/BioProtoc.3465.

Deng, N., Lv, Y., Bing, Q., Li, S., Han, B., Jiang, H., Yang, Q., Wang, X., Wu, P., Liu, Y., 2022. Inhibition of the nrf2 signaling pathway involved in imidacloprid-induced liver fibrosis in Coturnix japonica. Environ. Toxicol. 37, 2354–2365. https://doi.org/10.1002/tox.23601.

Deviche, P., Hurley, L.L., Fokidis, H.B., 2011. Chapter 2 - avian testicular structure, function, and regulation, in (Eds). In: Norris, D.O., Lopez, K.H. (Eds.), Hormones and reproduction of vertebrates. Academic Press, London, pp. 27–70. https://doi.org/10.1016/B978-0-12-374929-1.10002-2 (Eds).

EFSA (European Food Safety Authority), 2014. Conclusion on the peer review of the pesticide risk assessment of confirmatory data submitted for the active substance imidacloprid. EFSA J. 12, 20. https://doi.org/10.2903/j.efsa.2014.3741.

Eissa, O.S., 2004. Protective effect of vitamin c and glutathione against the histopathological changes induced by imidacloprid in the liver and testis of japanese quail. Egypt. J. Hosp. Med. 16, 39–54. https://doi.org/10.21608/ejhm.2004.18174.

Ensley, S.M., 2018. Neonicotinoids, in (Ed). In: Gupta, R.C. (Ed.), Veterinary toxicology. third edition). Academic Press, pp. 521–524. https://doi.org/10.1016/B978-0-12-811410-0.00040-4 (Ed).

Goulson, D., 2013. An overview of the environmental risks posed by neonicotinoid insecticides. J. Appl. Ecol. 50, 977–987. https://doi.org/10.1111/1365-2664.12111.

Hallmann, C.A., Foppen, R.P., Van Turnhout, C.A., De Kroon, H., Jongejans, E., 2014. Declines in insectivorous birds are associated with high neonicotinoid concentrations. Nature 511, 341–343. https://doi.org/10.1038/nature13531.

He, Y., Wang, L., Li, X., Zhao, H., 2020. The effects of chronic lead exposure on the ovaries of female juvenile japanese quails (*Coturnix japonica*): Developmental delay, histopathological alterations, hormone release disruption and gene expression disorder. Ecotoxicol. Environ. Saf. 205, 111338 https://doi.org/10.1016/j.ecoenv.2020.111338.

Ibrahim, H.Z., El-Banna, S.G., El Rafea, A.A., 2020. Acetamiprid, insecticide-induced oxidative damage on reproductive parameters male rats. Alex. J. Vet. Sci. 64. https://doi.org/10.5455/ajvs.78757.

Ibrahim, M.I.A., Ferreira, G.C.H., Venter, E.A., Botha, C.J., 2023. Cytotoxicity, morphological and ultrastructural effects induced by the neonicotinoid pesticide, imidacloprid, using a rat leydig cell line (lc-540). Environ. Toxicol. Pharmacol. 104, 104310 https://doi.org/10.1016/j.etap.2023.104310.

Jimenez-Lopez, J.C., 2017. Cytoskeleton: Structure, dynamics, function and disease. BoD–Books on Demand, InTech, Rijeka, Croatia. https://doi.org/10.5772/62622.

Johnson, L., Varner, D.D., Roberts, M.E., Smith, T.L., Keillor, G.E., Scrutchfield, W.L., 2000. Efficiency of spermatogenesis: a comparative approach. Anim. Reprod. Sci. 60-61, 471–480. https://doi.org/10.1016/S0378-4320(00)00108-1.

Kapoor, U., Srivastava, M.K., Srivastava, L.P., 2011. Toxicological impact of technical imidacloprid on ovarian morphology, hormones and antioxidant enzymes in female rats. Food Chem. Toxicol. 49, 3086–3089. https://doi.org/10.1016/j.fct.2011.09.009.

Kapoor, U., Srivastava, M.K., Trivedi, P., Garg, V., Srivastava, L.P., 2014. Disposition and acute toxicity of imidacloprid in female rats after single exposure. Food Chem. Toxicol. 68, 190–195. https://doi.org/10.1016/j.fct.2014.03.019.

Keles, H., Yalcin, A., Aydin, H., 2022. Protective effect of vitamin d on imidacloprid-induced testicular injury in rats. Arch. Med. Sci. 18, 1659-1665. https://doi.org/10.5114/aoms.2019.86776.

Kenfack, A., Guiekep, N., Ngoula, F., Vemo, B.N., Bouli, E., Pamo, E.T., 2018. Reproductive toxicity of acetamiprid in male guinea pig (Cavia porcellus). J. Anim. Sci. Vet. Med 3, 105–111 https://api.semanticscholar.org/CorpusID:92141230.

Kobir, M.A., Akter, L., Sultana, N., Pervin, M., Awal, M.A., Karim, M.R., 2023. Effects of imidacloprid-contaminated feed exposure on spermatogenic cells and leydig cells in testes of adult male rabbits (*Oryctolagus cuniculus*). Saudi J. Biol. Sci. 30, 103541 https://doi.org/10.1016/j.sjbs.2022.103541.

Kolasa, A., Marchlewicz, M., Wenda-Różewicka, L., Wiszniewska, B., 2011. Dht deficiency perturbs the integrity of the rat seminiferous epithelium by disrupting tight and adherens junctions. Folia Histochem. Et. Cytobiol. 49, 62–71. https://doi.org/10.5603/FHC.2011.0010.

Kong, D., Zhang, J., Hou, X., Zhang, S., Tan, J., Chen, Y., Yang, W., Zeng, J., Han, Y., Liu, X., 2017. Acetamiprid inhibits testosterone synthesis by affecting the mitochondrial function and cytoplasmic adenosine triphosphate production in rat leydig cells. Biol. Reprod. 96, 254–265. https://doi.org/10.1095/biolreprod.116.139550.

Kopecky, M., Semecky, V., Nachtigal, P., 2005. Vimentin expression during altered spermatogenesis in rats. Acta Histochem. 107, 279–289. https://doi.org/10.1016/j.acthis.2005.06.007.

Li, S., Zheng, X., Zhang, X., Yu, H., Han, B., Lv, Y., Liu, Y., Wang, X., Zhang, Z., 2021. Exploring the liver fibrosis induced by deltamethrin exposure in quails and elucidating the protective mechanism of resveratrol. Ecotoxicol. Environ. Saf. 207, 111501 https://doi.org/10.1016/j.ecoenv.2020.111501.

Lohiya, A., Kumar, V., Punia, J., 2019. Effect of imidacloprid on antioxidant status and histopathological changes in ovary and uterus of adult female wistar rats. Indian J. Anim. Res. 53, 1014-1019. https://doi.org/10.18805/ijar.B-3613.

Lopez-Antia, A., Ortiz-Santaliestra, M.E., Mougeot, F., Mateo, R., 2015. Imidacloprid-treated seed ingestion has lethal effect on adult partridges and reduces both breeding investment and offspring immunity. Environ. Res. 136, 97–107. https://doi.org/10.1016/j.envres.2014.10.023.

Lu, H., Zhang, C., Hu, Y., Qin, H., Gu, A., Li, Y., Zhang, L., Li, Z., Wang, Y., 2016. Mirna-200c mediates mono-butyl phthalate-disrupted steroidogenesis by targeting vimentin in leydig tumor cells and murine adrenocortical tumor cells. Toxicol. Lett. 241, 95–102. https://doi.org/10.1016/j.toxlet.2015.11.009.

Lv, Y., Bing, Q., Lv, Z., Xue, J., Li, S., Han, B., Yang, Q., Wang, X., Zhang, Z., 2020. Imidacloprid-induced liver fibrosis in quails via activation of the tgf-β1/smad pathway. Sci. Total Environ. 705, 135915 https://doi.org/10.1016/j.scitotenv.2019.135915.

Madekurozwa, M.C., 2007. An immunohistochemical study of the distribution of intermediate filaments in the ovary of the emu (*Dromaius novaehollandiae*). Anat., Histol., Embryol. 36, 336–342. https://doi.org/10.1111/j.1439-0264.2007.00771.x.

Madekurozwa, M.C., 2013. Post-hatch changes in the immunoexpression of desmin, smooth muscle actin and vimentin in the testicular capsule and interstitial tissue of the japanese quail (*Coturnix coturnix japonica*). Anat., Histol., Embryol 42, 369–378. https://doi.org/10.1111/ahe.12024.

Mahajan, L., Verma, P.K., Raina, R., Sood, S., 2018. Potentiating effect of imidacloprid on arsenic-induced testicular toxicity in wistar rats. BMC Pharmacol. Toxicol. 19 (1), 8. https://doi.org/10.1186/s40360-018-0239-9.

Marettová, E., Maretta, M., 2002. Demonstration of intermediate filaments in sheep ovary. Acta Histochem. 104, 431–434. https://doi.org/10.1078/0065-1281-00672.

Martinez, M., Macera, S., de Assis, G.F., Pinheiro, P.F.F., Almeida, C.C.D., Tirapelli, L.F., Martins, O.A., Mello-Júnior, W., Padovani, C.R., Martinez, F.E., 2009. Structural evaluation of the effects of chronic ethanol ingestion on the testis of Calomys callosus. Tissue Cell 41, 199–205. https://doi.org/10.1016/j.tice.2008.10.003.

Mikolić, A., Karačonji, I.B., 2018. Imidacloprid as reproductive toxicant and endocrine disruptor: Investigations in laboratory animals. Arch. Ind. Hyg. Toxicol. 69, 103–108. https://doi.org/10.2478/aiht-2018-69-3144.

Millot, F., Decors, A., Mastain, O., Quintaine, T., Berny, P., Vey, D., Lasseur, R., Bro, E., 2017. Field evidence of bird poisonings by imidacloprid-treated seeds: A review of incidents reported by the french sagir network from 1995 to 2014. Environ. Sci. Pollut. Res. 24, 5469–5485. https://doi.org/10.1007/s11356-016-8272-y.

Mineau, P., Palmer, C., 2013. The impact of the nation's most widely used insecticides on birds. American Bird Conservancy.

Mitra, A., Chatterjee, C., Mandal, F.B., 2011. Synthetic chemical pesticides and their effects on birds. Res. J. Environ. Toxicol. 5, 81–96. https://doi.org/10.3923/rjet.2011.81.96.

Mohanty, B., Pandey, S.P., Tsutsui, K., 2017. Thyroid disrupting pesticides impair the hypothalamic-pituitary-testicular axis of a wildlife bird, Amandava amandava. Reprod. Toxicol. 71, 32–41. https://doi.org/10.1016/j.reprotox.2017.04.006.

Moreira, D.R., de Souza, T.H.S., Galhardo, D., Puentes, S.M.D., Figueira, C.L., Silva, B.Gd, Chagas, Fd, Gigliolli, A.A.S., de Toledo, V.A.A., Ruvolo-Takasusaki, M.C.C., 2022. Imidacloprid induces histopathological damage in the midgut, ovary, and spermathecal stored spermatozoa of queens after chronic colony exposure. Environ. Toxicol. Chem. 41, 1637–1648. https://doi.org/10.1002/etc.5332.

Mourikes, V.E., Santacruz Márquez, R., Deviney, A., Neff, A.M., Laws, M.J., Flaws, J.A., 2023. Imidacloprid and its bioactive metabolite, desnitro-imidacloprid, differentially affect ovarian antral follicle growth, morphology, and hormone synthesis *in vitro*. Toxics 11, 349. https://doi.org/10.3390/toxics11040349.

Mzid, M., Ghlissi, Z., Salem, M.B., Khedir, S.B., Chaabouni, K., Ayedi, F., Sahnoun, Z., Hakim, A., Rebai, T., 2018. Chemoprotective role of ethanol extract of Urtica urens l. Against the toxicity of imidacloprid on endocrine disruption and ovarian morphometric in female rats, gc/ms analysis. Biomed. Pharmacother. 97, 518–527. https://doi.org/10.1016/j.biopha.2017.10.150.

Nabiuni, M., Parivar, K., Noorinejad, R., Falahati, Z., Khalili, F., Karimzadeh, L., 2015. The reproductive side effects of imidacloprid in pregnant wistar rat. Int. J. Cell. Mol. Biotechnol. Abbr. 8, 9. https://doi.org/10.5899/2015/ijcmb-00017.

Nad, P., Massanyi, P., Skalicka, M., Korenekova, B., Cigankova, V., Almasiova, V., 2007. The effect of cadmium in combination with zinc and selenium on ovarian structure in japanese quails. J. Environ. Sci. Health Part A 42, 2017–2022. https://doi.org/10.1080/10934520701629716.

Nimako, C., Ikenaka, Y., Akoto, O., Fujioka, K., Taira, K., Arizono, K., Kato, K., Takahashi, K., Nakayama, S.M.M., Ichise, T., Ishizuka, M., 2021. Simultaneous quantification of imidacloprid and its metabolites in tissues of mice upon chronic low-dose administration of imidacloprid. J. Chromatogr. A 1652, 462350. https://doi.org/10.1016/j.chroma.2021.462350.

OECD, 2022. Test no. 425: Acute oral toxicity: Up-and-down procedure. doi:https://doi.org/10.1787/9789264071049-en.

Onagbesan, O., Bruggeman, V., Decuypere, E., 2009. Intra-ovarian growth factors regulating ovarian function in avian species: a review. Anim. Reprod. Sci. 111, 121–140. https://doi.org/10.1016/j.anireprosci.2008.09.017.

Ozegbe, P., Aire, T.A., Madekurozwa, M.-C., Soley, J.T., 2008a. Morphological and immunohistochemical study of testicular capsule and peritubular tissue of emu (*Dromaius novaehollandiae*) and ostrich (*Struthio camelus*). Cell Tissue Res. 332, 151–158. https://doi.org/10.1007/s00441-007-0515-2.

Ozegbe, P.C., Aire, T.A., Madekurozwa, M.C., Soley, J.T., 2008b. Morphological and immunohistochemical study of testicular capsule and peritubular tissue of emu (Dromaius novaehollandiae) and ostrich (Struthio camelus). Cell Tissue Res. 332, 151–158. https://doi.org/10.1007/s00441-007-0515-2.

Pandey, S.P., Mohanty, B., 2015. The neonicotinoid pesticide imidacloprid and the dithiocarbamate fungicide mancozeb disrupt the pituitary–thyroid axis of a wildlife bird. Chemosphere 122, 227–234. https://doi.org/10.1016/j.chemosphere.2014.11.061.

Percie du Sert, N., Ahluwalia, A., Alam, S., Avey, M.T., Baker, M., Browne, W.J., Clark, A., Cuthill, I.C., Dirnagl, U., Emerson, M., Garner, P., Holgate, S.T., Howells, D.W., Hurst, V., Karp, N.A., Lazic, S.E., Lidster, K., MacCallum, C.J., Macleod, M., Pearl, E.J., Petersen, O.H., Rawle, F., Reynolds, P., Rooney, K., Sena, E. S., Silberberg, S.D., Steckler, T., Würbel, H., 2020. Reporting animal research: Explanation and elaboration for the arrive guidelines 2.0. PLOS Biol. 18, e3000411 https://doi.org/10.1371/journal.pbio.3000411.

Posthuma-Doodeman, C., 2008. Environmental risk limits for imidacloprid. RIVM Letter report 601716018.

Prasad, S., Tiwari, M., Pandey, A.N., Shrivastav, T.G., Chaube, S.K., 2016. Impact of stress on oocyte quality and reproductive outcome. J. Biomed. Sci. 23, 36. https://doi.org/10.1186/s12929-016-0253-4.

Qin, L., Du, Z.-H., Zhu, S.-Y., Li, X.-N., Li, N., Guo, J.-A., Li, J.-L., Zhang, Y., 2015. Atrazine triggers developmental abnormality of ovary and oviduct in quails (*Coturnix coturnix coturnix*) via disruption of hypothalamo-pituitary-ovarian axis. Environ. Pollut. 207, 299–307. https://doi.org/10.1016/j.envpol.2015.09.044.

Rodler, D., Stein, K., Korbel, R., 2015. Observations on the right ovary of birds of prey: A histological and immunohistochemical study. Anat., Histol., Embryol. 44, 168–177. https://doi.org/10.1111/ahe.12121.

Rogers, K.H., McMillin, S., Olstad, K.J., Poppenga, R.H., 2019. Imidacloprid poisoning of songbirds following a drench application of trees in a residential neighborhood in california, USA. Environ. Toxicol. Chem. 38, 1724–1727. https://doi.org/10.1002/etc.4473.

Saber, T.M., Arisha, A.H., Abo-Elmaaty, A.M.A., Abdelgawad, F.E., Metwally, M.M.M., Saber, T., Mansour, M.F., 2021. Thymol alleviates imidacloprid-induced testicular toxicity by modulating oxidative stress and expression of steroidogenesis and apoptosis-related genes in adult male rats. Ecotoxicol. Environ. Saf. 221, 112435 https://doi.org/10.1016/j.ecoenv.2021.112435.

Schindelin, J., Arganda-Carreras, I., Frise, E., Kaynig, V., Longair, M., Pietzsch, T., Preibisch, S., Rueden, C., Saalfeld, S., Schmid, B., 2012. Fiji: An open-source platform for biological-image analysis. v1.53t (version 1.53t). Nat. Methods 9, 676–682. https://doi.org/10.1038/nmeth.2019.

SERA, 2005. Imidacloprid-human health and ecological risk assessment–appendices. Fayetteville, new york: Syracuse environmental research associates.

Sevim, Ç., Akpınar, E., Aksu, E.H., Ömür, A.D., Yıldırım, S., Kara, M., Bolat, İ., Tsatsakis, A., Mesnage, R., Golokhvast, K.S., Uzunçakmak, S.K., Ersoylu, R.N., 2023. Reproductive effects of s. Boulardii on sub-chronic acetamiprid and imidacloprid toxicity in male rats. Toxics 11, 170. https://doi.org/10.3390/toxics11020170.

Shimomura, M., Yokota, M., Ihara, M., Akamatsu, M., Sattelle, D.B., Matsuda, K., 2006. Role in the selectivity of neonicotinoids of insect-specific basic residues in loop d of the nicotinic acetylcholine receptor agonist binding site. Mol. Pharmacol. 70, 1255–1263. https://doi.org/10.1124/mol.106.026815.

da Silveira Firmiano, E.M., Machado-Santos, C., Serra-Campos, A.O., Maria de Sousa, B., Pinheiro, N.L., do Nascimento, A.A., 2021. Histological study and immunohistochemical location of cytoskeletal proteins in the ovaries of the three species of lizards of the family leiosauridae (*reptilia squamata*). Tissue Cell 68, 101477. https://doi.org/10.1016/j.tice.2020.101477.

Singh, S.R., Kadioglu, H., Patel, K., Carrier, L., Agnetti, G., 2020. Is desmin propensity to aggregate part of its protective function? Cells 9, 491. https://doi.org/10.3390/cells9020491.

Sohel, M.M.H., Akyuz, B., Konca, Y., Arslan, K., Sariozkan, S., Cinar, M.U., 2019. Oxidative stress modulates the expression of apoptosis-associated micrornas in bovine granulosa cells *in vitro*. Cell Tissue Res. 376, 295–308. https://doi.org/10.1007/s00441-019-02990-3.

Sood, P., 2023. Imidacloprid induced reproductive toxicity in female albino rats. Indian J. Entomol. 343–347. https://doi.org/10.55446/IJE.2022.534.

Suliman, Khan, A., Shah, S.S.A., Gulfam, N., Khisroon, M., Zahoor, M., 2020. Toxicity evaluation of pesticide chlorpyrifos in male japanese quails (Coturnix japonica). Environ. Sci. Pollut. Res. 27, 25353–25362. https://doi.org/10.1007/s11356-020-08953-4.

Talpur, F.N., Unar, A., Bhatti, S.K., Alsawalha, L., Fouad, D., Bashir, H., Afridi, H.I., Ataya, F.S., Jefri, O.A., Bashir, M.S., 2023. Bioremediation of neonicotinoid pesticide, imidacloprid, mediated by bacillus cereus. Bioengineering 10, 951. https://doi.org/10.3390/bioengineering10080951.

Tokumoto, J., Danjo, M., Kobayashi, Y., Kinoshita, K., Omotehara, T., Tatsumi, A., Hashiguchi, M., Sekijima, T., Kamisoyama, H., Yokoyama, T., 2013. Effects of exposure to clothianidin on the reproductive system of male quails. J. Vet. Med. Sci. 75, 755–760. https://doi.org/10.1292/jvms.12-0544.

Tomizawa, M., Casida, J.E., 2005. Neonicotinoid insecticide toxicology: Mechanisms of selective action. Annu. Rev. Pharmacol. Toxicol. 45, 247. https://doi.org/10.1146/annurev.pharmtox.45.120403.095930.

Van den Hurk, R., Dijkstra, G., Van Mil, F., Hulshof, S., van den Ingh, T.S., 1995. Distribution of the intermediate filament proteins vimentin, keratin, and desmin in the bovine ovary. Mol. Reprod. Dev. 41, 459–467. https://doi.org/10.1002/mrd.1080410408.

Van Nassauw, L., Callebaut, M., 1991. Structural and immunohistochemical aspects of the postovulatory follicle in japanese quail. Anat. Rec. 229, 27–30. https://doi.org/10.1002/ar.1092290105.

Vohra, P., Khera, K.S., 2016. Effect of imidacloprid on reproduction of female albino rats in three generation study. J. Vet. Sci. Technol. 7, 1000340. https://doi.org/10.4172/2157-7579.1000340.

Wang, Y., Fu, Y., Wang, Y., Lu, Q., Ruan, H., Luo, J., Yang, M., 2022. A comprehensive review on the pretreatment and detection methods of neonicotinoid insecticides in food and environmental samples. Food Chem.: X 15, 100375. https://doi.org/10.1016/j.fochx.2022.100375.

Yan, M., Shi, Y., Wang, Y., Wang, C., Zhou, J., Quan, C., Liu, C., Yang, K., 2013. Effects of p,p′-dde on the mrna and protein expressions of vimentin, n-cadherin and fshr in rats testes: an in vivo and in vitro study. Environ. Toxicol. Pharmacol. 35, 486–494. https://doi.org/10.1016/j.etap.2013.02.008.

Yang, L., Shen, Q., Zeng, T., Li, J., Li, W., Wang, Y., 2020. Enrichment of imidacloprid and its metabolites in lizards and its toxic effects on gonads. Environ. Pollut. 258, 113748 https://doi.org/10.1016/j.envpol.2019.113748.

Zhang, Q., Li, Z., Chang, C.H., Lou, J.L., Zhao, M.R., Lu, C., 2018. Potential human exposures to neonicotinoid insecticides: a review. Environ. Pollut. 236, 71–81. https://doi.org/10.1016/j.envpol.2017.12.101.

Zhao, G.-p, Li, J.-w, Yang, F.-w, Yin, X.-f, Ren, F.-z, Fang, B., Pang, G.-f, 2021. Spermiogenesis toxicity of imidacloprid in rats, possible role of cyp3a4. Chemosphere 282, 131120. https://doi.org/10.1016/j.chemosphere.2021.131120.

Zhao, G.P., Yang, F.W., Li, J.W., Xing, H.Z., Ren, F.Z., Pang, G.F., Li, Y.X., 2020. Toxicities of neonicotinoid-containing pesticide mixtures on nontarget organisms. Environ. Toxicol. Chem. 39, 1884–1893. https://doi.org/10.1002/etc.4842.

Zhou, F., Shi, L.-B., Zhang, S.-Y., 2017. Ovarian fibrosis: a phenomenon of concern. Chin. Med. J. 130, 365–371. https://doi.org/10.4103/0366-6999.198931.